EFFECTIVE FIELD THEORY OF THE ELECTROWEAK SECTOR

BY

HARRISON E MEBANE

DISSERTATION

Submitted in partial fulfillment of the requirements
for the degree of Doctor of Philosophy in Physics
in the Graduate College of the
University of Illinois at Urbana-Champaign, 2013

Urbana, Illinois

Doctoral Committee:

Associate Professor Timothy Stelzer, Chair
Professor Scott Willenbrock, Director of Research
Assistant Professor Mark Neubauer
Professor James Eckstein

Abstract

Effective field theory is a model-independent way to search for indirect effects of new physics. It has many advantages over the traditional anomalous couplings framework. In particular, gauge invariance makes possible the calculation of loop corrections. Furthermore, the issue of unitarity violation is shown to be irrelevant in an effective field theory.

There are nine dimension-six operators which generate corrections to precision electroweak quantities through gauge boson propagators. I start with an analysis involving just two operators contributing at one loop in which I show that loop calculations, and the renormalization program in particular, can be carried out in a straightforward manner using effective field theory. I compare this to previous analyses and show that the methods presented here yield more accurate bounds on loop-level operator coefficients.

I finish with a global analysis of the full set of nine operators. Bounds are presented on the linearly-independent combinations of the operators. The four operators which affect precision electroweak observables at tree-level are shown to absorb all divergences from the five operators contributing only at loop-level. The bounds are found to be considerably weaker than existing bounds from collider data.

To my parents,

and to Mica.

Acknowledgments

I must begin by thanking my advisor, Scott Willenbrock. I cannot imagine a better person to have guided me intellectually through the past few years, and I am grateful for his patience and understanding throughout all of my graduate school endeavors. I would also like to thank Tim Stelzer, who is at once a shining example of what a college professor should be, and an expert lunch conversationalist. I am also indebted to my colleagues Will Link, Rob Putman, Nick Greiner, Celine Degrande, Olivier Mattelaer, and especially Cen Zhang, for answering my sometimes incoherent questions and offering advice when needed.

I owe many thanks to the friends who have entertained and enriched me for the past five years. In no particular order, I would like to thank: Brian, for all of the hours spent watching sports and hanging out; my Tuesday poker buddies, for always giving me something fun to do during the grind of the week; the fine people of the French department, for taking me in as a friend when I arrived here; the MATESL people, for also taking me in, and for all the delicious potlucks; the Classics people for also also taking me in, and for many hours of games and laughs; Centaur of Attention, the finest of the Blind Pig trivia teams; and Kayla and Darby, for all the awesome double dates.

Thank you to my lovely fiancée, Mica, for keeping me laughing and having fun through five years of graduate school. I have done so many interesting things and met so many interesting people since we moved here; I think I owe you for almost all of that. I would also like to thank the other part of my Champaign family, Bodger the French Bulldog. Thank you, Bodger, for always farting during serious moments of conversation, making strange noises, and generally being a lovable doofus.

Thank you to my brother, Palmer, for being you. You manage to walk the fine line between normal-functioning human and eccentric genius with aplomb, which is something few can say. Finally, I would not be where I am today, literally or figuratively, without my parents. Your commitment to my education from day one is the reason I have made it to this point. I may never know all of the sacrifices you have made on my behalf, but they are appreciated, nonetheless.

This work was supported by NSF grant PHY10-68326, Department of Energy contract No. DE-FG02-91ER40677, the University of Illinois Department of Physics, and the University of Illinois Graduate College.

Table of Contents

List of Abbreviations

TGC	Triple gauge coupling
VEV	Vacuum Expectation Value
LHC	Large Hadron Collider
RGE	Renormalization Group Equation

List of Symbols

$\phi = \begin{pmatrix} -i\phi^+ \\ \frac{1}{\sqrt{2}}(v + h - i\phi^0) \end{pmatrix}$	Higgs doublet
$\hat{W}_{\mu\nu} = ig\frac{\sigma^I}{2}(\partial_\mu W^I_\nu - \partial_\nu W^I_\mu + g\epsilon_{IJK}W^J_\mu W^K_\nu)$	W field strength tensor
$\hat{B}_{\mu\nu} = \frac{ig'}{2}(\partial_\mu B_\nu - \partial_\nu B_\mu)$	B field strength tensor
$D_\mu = \partial_\mu - ig'YB_\mu - ig\frac{\sigma^I}{2}W^I_\mu$	Covariant derivative

Chapter 1

Introduction

The standard model is the result of many years of effort by multiple generations of physicists. It represents our best attempt at explaining the way the universe works at high energies and small length scales. Through many years of high-energy collider experiments and low-energy precision measurements, the standard model has been tested and has passed with flying colors. However, we know that the standard model cannot be the whole story. It fails to explain several observed phenomena, including dark matter and neutrino mass. It also provides no answer to some deeper challenges, such as the hierarchy problem, which is the issue of why the Higgs boson mass is so small in the face of apparently large quantum corrections. We expect, then, that there is physics beyond the standard model. Because it has not been directly observed, we may assume that it lies beyond the energy domain of past experiments; it is generally assumed to be of order 1 TeV in order to stabilize the electroweak scale, but it could be higher.

There are numerous theories for physics beyond the standard model: supersymmetry, extra dimensions, technicolor, and many more. Each of these theories has a different experimental signature and must be looked for separately in experimental data. It is desirable, then, to express the effects of new physics in a model-independent way, in order to standardize the language of beyond-the-standard-model physics. This dissertation will achieve this goal through the use of effective field theory.

An effective field theory is a low-energy approximation of a theory containing fields of high mass. At low energies, particles of sufficiently high mass cannot be observed directly, but their indirect effects can be measured. An effective field theory provides a way to quantify these effects without the need to include heavy particles in the theory. Heavy fields are "integrated out" of the Lagrangian of the full theory, leaving behind additional interactions between the lighter fields.

In order to make this procedure more concrete, consider the standard model. As a renormalizable theory, it contains only interactions with energy dimension[1] four or less.[2] Now suppose that there is some as-yet-undiscovered particle with a mass above current experimental limits. In the effective field theory framework,

[1] Because we are using natural units, *energy dimension* is redundant. From here on, we will just say *dimension*.

[2] In fact, all standard-model interactions have dimension four except for the quadratic term in the Higgs potential, which is dimension two.

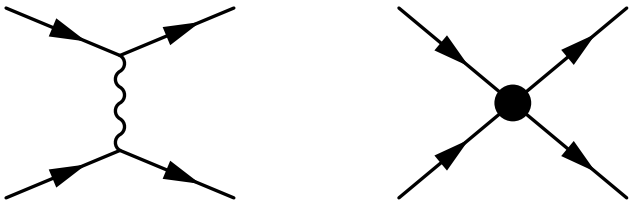

Figure 1.1: In the Fermi model, the W- or Z-mediated standard model process (*left*) becomes an effective four-fermion interaction (*right*).

when we integrate out this heavy field, we are taking the heavy particle's mass to be large compared to experimentally accessible energies; this shrinks the propagator down to a point, resulting in new interactions between the standard model fields. We refer to these interaction terms as effective operators.

An excellent illustration of this process is the Fermi model for the weak interaction. Fermi explained beta decay in terms of a four-fermion contact interaction, adding a term of the following form to the Lagrangian[3]

$$\mathcal{L}_{fermi} = \frac{G_F}{\sqrt{2}} \left(\bar{u}\gamma_\mu(1-\gamma_5)d\right)\left(\bar{e}\gamma^\mu(1-\gamma_5)\nu_e\right) \tag{1.1}$$

Note that the Fermi interaction is a dimension-six operator. This is just a low-energy approximation for the weak process $d \to u + e^- + \bar{\nu}_e$ (see Fig. 1.1). If we calculate the amplitude for this process in the full weak theory, we get

$$\mathcal{M} = \frac{g^2}{2}\left(\bar{u}_u\gamma_\mu\frac{1}{2}(1-\gamma_5)u_d\right)\frac{i}{p^2-m_W^2+i\epsilon}\left(g^{\mu\nu}-\frac{p^\mu p^\nu}{m_W^2}\right)\left(\bar{u}_e\gamma_\nu\frac{1}{2}(1-\gamma_5)v_{\nu_e}\right) \tag{1.2}$$

In the low-energy limit, this reduces to

$$\lim_{p^2\ll m_W^2}\mathcal{M} = \frac{-ig^2}{8m_W^2}\left(\bar{u}_u\gamma_\mu(1-\gamma_5)u_d\right)\left(\bar{u}_e\gamma^\mu(1-\gamma_5)v_{\nu_e}\right) \tag{1.3}$$

This corresponds directly to Fermi's contact interaction, with $\frac{G_F}{\sqrt{2}} = \frac{g^2}{8m_W^2}$. At low energies, we see a four-fermion contact interaction whose strength is suppressed by the square of the W-boson mass. This is a general feature of effective field theories; operators of dimension greater than four will be suppressed by inverse powers of the mass scale of new physics.

Effective field theories have a variety of desirable characteristics:

- They satisfy standard model $SU(3)\times SU(2)\times U(1)$ gauge symmetry. This provides a useful check on calculations.

[3]Fermi did not know that the actual weak interaction has V-A coupling. I have included the left-handed projection $(1-\gamma_5)$ in the expression for easier comparison with the standard model expression.

- They reduce to the standard model in the appropriate limit.
- They provide a complete, model-independent representation of physics beyond the standard model.
- There is a well-defined procedure for handling divergences generated by loop diagrams, which are necessary for next-to-leading-order corrections.

When creating an effective field theory, we can either start with a model and integrate out heavy degrees of freedom to get a low-energy theory, or we can start with a low-energy theory and include all operators up to a given dimension which satisfy standard model gauge symmetry. The latter approach is more desirable in the present environment, as it offers a model-independent way of expressing the indirect effects of new physics. The most general effective field theory for physics beyond the standard model can be written in the following way

$$\mathcal{L}_{eff} = \mathcal{L}_{SM} + \frac{1}{\Lambda}\sum_i c_i \mathcal{O}_i^{(5)} + \frac{1}{\Lambda^2}\sum_j c_j \mathcal{O}_j^{(6)} + \cdots \tag{1.4}$$

where Λ is the mass scale of new physics, the c_i are dimensionless constants, and the $\mathcal{O}_i^{(d)}$ are operators of dimension d. Note that the standard model Lagrangian has dimension four, so the Λ's are necessary from a dimensional-analysis standpoint. At low energy, an operator's contribution to the cross section will scale inversely with its dimension, as lower-dimensional operators are less suppressed by powers of Λ. In this dissertation, we will focus on electroweak operators of dimension six.[4]

This dissertation has three sections. In Chapter 2, I discuss electroweak effective field theory and examine the effects of effective operators on a tree-level amplitude. In Chapter 3, I compute bounds on a pair of effective operators using precision electroweak data and compare them to other bounds in the literature. In Chapter 4, I compute bounds on a complete set of nine electroweak operators, again using precision electroweak data.

[4]There is only one dimension-five operator. It generates neutrino masses, but it is not relevant to analyses herein.

Chapter 2

Electroweak Effective Field Theory

In Chapter 1, the Fermi model was used as an example of an effective field theory. From our point of view, the Fermi model represents a well-defined approximation to the full electroweak theory. From Fermi's view, this was an effort to explain new physics in a calculable framework. Today, we find ourselves in a similar position to Fermi: we know new physics exists beyond the standard model, but we need a way to describe it in a model-independent way. We can do this in the effective field theory framework by writing down all interactions which satisfy Lorentz and gauge symmetries, up to a given dimension.

Given that there is only one dimension-five operator, compiling all operators up to dimension six is adequate as a first-order correction to the standard model. After using equations of motion to remove redundant operators, one finds 59 independent dimension-six operators [1]. As only some of these operators can be bounded by any given set of data, it makes sense to limit one's consideration to a subset of operators. In this paper, we will deal with those operators which contain only electroweak bosons. We will also require that the operators be invariant with respect to charge conjugation and parity. As with any multidimensional space, we must pick a basis of such operators; in this dissertation, we will use the set given in Ref. [2].

2.1 Electroweak Effective Operators

The effective operators treated here all affect electroweak observables through corrections to gauge boson propagators or triple gauge couplings (TGCs). As the main results of this dissertation depend on self-energy corrections, we will group the operators into three different categories, based upon their effect on gauge boson propagators.

The first four operators contribute to gauge boson self energies at tree-level

$$\mathcal{O}_{BW} = \phi^\dagger \hat{W}^{\mu\nu} \hat{B}_{\mu\nu} \phi \tag{2.1a}$$

$$\mathcal{O}_{\phi,1} = (D_\mu \phi)^\dagger \phi \, \phi^\dagger (D^\mu \phi) \tag{2.1b}$$

$$\mathcal{O}_{DW} = D^\mu \hat{W}^{\nu\rho} D_\mu \hat{W}_{\nu\rho} \tag{2.1c}$$

$$\mathcal{O}_{DB} = \partial^\mu \hat{B}^{\nu\rho} \partial_\mu \hat{B}_{\nu\rho} \tag{2.1d}$$

Note that $\mathcal{O}_{DW}$ and $\mathcal{O}_{BW}$–when the Higgs doublets take their vacuum expectation values (VEVs)–also contribute to anomalous TGCs.

The next five operators contribute to the gauge boson propagators only at loop-level

$$\mathcal{O}_{WWW} = \mathrm{Tr}\, \hat{W}^{\mu}{}_{\nu} \hat{W}^{\nu}{}_{\rho} \hat{W}^{\rho}{}_{\mu} \tag{2.2a}$$

$$\mathcal{O}_{W} = (D_\mu \phi)^\dagger \, \hat{W}^{\mu\nu} \, (D_\nu \phi) \tag{2.2b}$$

$$\mathcal{O}_{B} = (D_\mu \phi)^\dagger \, \hat{B}^{\mu\nu} \, (D_\nu \phi) \tag{2.2c}$$

$$\mathcal{O}_{WW} = \phi^\dagger \hat{W}^{\mu\nu} \hat{W}_{\mu\nu} \phi \tag{2.2d}$$

$$\mathcal{O}_{BB} = \phi^\dagger \hat{B}^{\mu\nu} \hat{B}_{\mu\nu} \phi \tag{2.2e}$$

Note that $\mathcal{O}_{WWW}$, $\mathcal{O}_{W}$, and $\mathcal{O}_{B}$, all contribute to anomalous TGCs. It appears as though $\mathcal{O}_{WW}$ and $\mathcal{O}_{BB}$ would also contribute to boson self energies at tree-level; however, when the Higgs doublets take their VEVs, the operators have the exact same form as the standard model gauge kinetic terms. Thus, purely bosonic interactions can be absorbed into a redefinition of the gauge couplings g and g' and the gauge fields W_μ and B_μ. The effects of these operators are limited to interactions involving Higgs fields. The operator $\mathcal{O}_{WW}$ does not contribute to anomalous TGCs for the same reason.

The final pair of operators are Higgs-only operators

$$\mathcal{O}_{\phi}^{(1)} = \frac{1}{2} \phi^\dagger \phi \, (D^\mu \phi)^\dagger \, (D_\mu \phi) \tag{2.3a}$$

$$\mathcal{O}_{\phi}^{(2)} = \frac{1}{3} \left(\phi^\dagger \phi\right)^3 \tag{2.3b}$$

These operators will not enter into our analysis because, at the one-loop level, their effects can be absorbed into a renormalization of parameters in the Higgs potential.

2.2 Anomalous Couplings

In the days before widespread acceptance of modern electroweak theory, deviations from the theory were measured via anomalous couplings. Like effective operators, anomalous couplings represent deviations from, or additions to, the interactions of the standard model; however, they differ in that they do not respect $SU(2)_L$ gauge invariance, and they do not have an inherent mass scale [3]. These differences result in a variety of limitations relative to an effective field theory.

Often, anomalous couplings are written in the form of an "interaction Lagrangian," which substitutes physical fields (e.g., W_μ^+) for gauge-invariant quantities (e.g., $W^{\mu\nu}$) [2]

$$\mathcal{L} = ig_{WWV}\left(g_1^V(W_{\mu\nu}^+W^{-\mu} - W^{+\mu}W_{\mu\nu}^-)V^\nu + \kappa_V W_\mu^+ W_\nu^- V^{\mu\nu} + \frac{\lambda_V}{m_W^2}W_\mu^{\nu+}W_\nu^{-\rho}V_\rho^\mu + \cdots\right) \tag{2.4}$$

Here V_μ corresponds to either a photon or a Z boson and g_{WWV} corresponds to the standard model triple-boson coupling. This approach is fine for tree-level calculations, but one runs into problems when calculating loop diagrams in an anomalous couplings framework. Specifically, the final operator in (2.4) has dimension six. In order to absorb loop divergences involving this operator, other dimension-six operators will be needed. In an effective field theory framework, these operators are readily available; in an anomalous couplings framework, the procedure is unclear. Another issue is that of unitarity violation, which will be discussed in Section 2.4.

It should be noted that the coefficients in (2.4) can be directly related to coefficients of dimension-six operators. In terms of the coefficients of the operators presented in Section 2.1, we have

$$g_1^Z = 1 + c_W\frac{m_Z^2}{2\Lambda^2} \tag{2.5a}$$

$$\kappa_\gamma = 1 + (c_B + c_W)\frac{m_W^2}{2\Lambda^2} \tag{2.5b}$$

$$\kappa_Z = 1 + \left(c_W - s^2(c_B + c_W)\right)\frac{m_Z^2}{2\Lambda^2} \tag{2.5c}$$

$$\lambda_\gamma = \lambda_Z = \frac{3m_W^2g^2}{2\Lambda^2}c_{WWW} \tag{2.5d}$$

where s is the sine of the weak mixing angle. Note that g_1^γ is fixed at unity by electromagnetic gauge invariance. The above expressions highlight the advantage of gauge-symmetric operators. We have reduced the number of independent coefficients from five to three. Gauge symmetry forces relationships between the operators which are not apparent in the Lagrangian in (2.4). The operators $\mathcal{O}_{BW}$ and $\mathcal{O}_{DW}$ also affect the anomalous couplings above, but because they affect the boson propagators as well, their tree-level effects

cannot be fully expressed through anomalous TGCs. Using equations of motion, we find that these operators are equivalent to some linear combination of $\mathcal{O}_W$, $\mathcal{O}_B$, and $\mathcal{O}_{WWW}$, plus operators containing both bosons and fermions. Because $\mathcal{O}_{BW}$ and $\mathcal{O}_{DW}$ affect the boson propagators at tree-level, they are much more tightly constrained than $\mathcal{O}_W$, $\mathcal{O}_B$, and $\mathcal{O}_{WWW}$, so we are justified in only considering the latter in investigations of anomalous TGCs.

Often, the boson interactions in (2.4) will be written explicitly in momentum-space, in which case we refer to them as vertex functions. For example, we might write the first term in (2.4) as

$$\Gamma^{\mu\nu\rho} = f_1^V(q^2)\left\{q^\nu \eta^{\mu\rho} - q^\mu \eta^{\nu\rho}\right\} \tag{2.6}$$

where the indices μ, ν, and ρ, correspond to the W^+, W^-, and neutral boson, respectively. Notice that I have promoted the constant coefficient g_1^V to a function of momentum $f_1^V(q^2)$. The function f_1^V is called a form factor. The rationale for form factors will be discussed in Section 2.4.

2.3 Bounds from Boson Pair Production

We noted in Section 2.2 that the operators $\mathcal{O}_W$, $\mathcal{O}_B$, and $\mathcal{O}_{WWW}$, affect TGCs at tree-level. In this section, we will look at bounds obtained on these operators from boson pair production. These operators also affect gauge boson self energies, but at loop-level, so the TGC effects are dominant. Furthermore, there are tree-level effects from the operators in (2.1), but these operators are already highly constrained, so we will ignore their effects for now.

Corrections to the $WW\gamma$ and WWZ vertices are

$$\begin{aligned}\Delta\Gamma^{WW\gamma}_{\mu\nu\rho} = {} & \frac{(c_W + c_B)}{\Lambda^2}\frac{m_W^2}{2} e\left(q_\mu \eta_{\nu\rho} - q_\nu \eta_{\mu\rho}\right) + \frac{c_{WWW}}{\Lambda^2}\frac{3g^2}{2} e\left(q_\mu k_\rho k'_\nu - q_\nu k_\mu k'_\rho + \right. \\ & \left. \left(q_\nu (k\cdot k') - k'_n u (q\cdot k)\right)\eta_{\mu\rho} + \left(k'_\rho (q\cdot k) - k_\rho (q\cdot k')\right)\eta_{\mu\nu} + \left(k_\mu (q\cdot k') - q_\mu (k\cdot k')\right)\eta_{\nu\rho}\right) \quad (2.7a)\end{aligned}$$

$$\begin{aligned}\Delta\Gamma^{WWZ}_{\mu\nu\rho} = {} & \frac{c_B}{\Lambda^2}\frac{s}{c}\frac{m_W^2}{2} e\left(q_\nu \eta_{\mu\rho} - q_\mu \eta_{\nu\rho}\right) + \frac{c_W}{\Lambda^2}\frac{1}{c}\frac{m_W^2}{2} g\left((k'-k)_\rho \eta_{\mu\nu} + k_\mu \eta_{\nu\rho} - k'_\nu \eta_{\mu\rho}\right. \\ & \left. + c^2\left(q_\mu \eta_{\nu\rho} - q_\nu \eta_{\mu\rho}\right)\right) + \frac{c_{WWW}}{\Lambda^2}\frac{3c}{2} g^3\left(q_\mu k_\rho k'_\nu - q_\nu k_\mu k'_\rho + \right. \\ & \left. \left(q_\nu (k\cdot k') - k'_n u (q\cdot k)\right)\eta_{\mu\rho} + \left(k'_\rho (q\cdot k) - k_\rho (q\cdot k')\right)\eta_{\mu\nu} + \left(k_\mu (q\cdot k') - q_\mu (k\cdot k')\right)\eta_{\nu\rho}\right) \quad (2.7b)\end{aligned}$$

From here it is straightforward to compute corrections to W-pair-production cross sections in terms of $\mathcal{O}_W$, $\mathcal{O}_B$, and $\mathcal{O}_{WWW}$, compare to data, and compute bounds. For simplicity, here we will use available bounds on anomalous couplings to arrive at bounds on effective operator coefficients.

In the previous section, we saw that the anomalous couplings g_1^Z, κ_Z, κ_γ, λ_Z, and λ_γ, can be expressed in terms of the effective operator coefficients c_W, c_B, and c_{WWW}. Using anomalous coupling bounds from Ref. [4], we arrive at the following constraints

$$\frac{c_W}{\Lambda^2} = -3.5 \pm 4.9 \text{ TeV}^{-2} \tag{2.8a}$$

$$\frac{c_B}{\Lambda^2} = 3.5 \pm 11 \text{ TeV}^{-2} \tag{2.8b}$$

$$\frac{c_{WWW}}{\Lambda^2} = -6.9 \pm 5.0 \text{ TeV}^{-2} \tag{2.8c}$$

Note that while anomalous couplings are dimensionless, effective operator bounds are dependent upon the mass scale Λ. We have just shown that anomalous couplings are compatible with effective field theory at tree-level when treated as constants. We will see in the next section that this latter condition is not always satisfied.

2.4 Unitarity

The scattering matrix, or S-matrix, is a matrix connecting the initial and final states of a scattering process. The entries of the S-matrix, or scattering amplitudes, can be used to determine the cross section of any given interaction between fields. Because such processes are inherently probabilistic, the S-matrix must be unitary. This unitarity implies a bound on scattering amplitudes and cross sections. Using partial wave analysis, we can determine the unitarity bound for any 2-to-2 scattering process

$$\sum_{\lambda_3,\lambda_4} \int dPS_2 \, |T^{in}|^2 \leq 24\pi \tag{2.9}$$

For the parton process $q\bar{q} \to W^+W^-$, this gives the following cross section bound

$$\sigma \leq \frac{2\pi}{\hat{s}} \tag{2.10}$$

where $\hat{s}$ is the square of the center-of-mass energy for the parton process. A full derivation of this inequality can be found in Appendix A.

One concern when dealing with higher-dimensional operators is the violation of unitarity at high energies. A cross section involving a dimension-six operator, for example, can contain a factor of $\hat{s}/\Lambda^2$. As energy increases, such a cross section will exceed the standard model cross section, possibly violating unitarity at sufficiently high energy.

As an example, consider W-pair production. The analytic parton-level cross section for producing two transverse W's, including the effect of the operator $\mathcal{O}_{WWW}$, is

$$\begin{aligned}\frac{d\sigma}{d\hat{t}} = \frac{\pi}{12}\frac{\alpha^2}{s^4}\frac{1}{\beta^4}\frac{\hat{u}\hat{t}-m_W^4}{\hat{s}^4}\Bigg[&\frac{1}{\hat{t}^2}(\hat{u}^2+\hat{t}^2-2m_W^4) \\ &+\frac{\hat{s}^2}{8\gamma^4}\left(\frac{1}{(\hat{s}-m_Z^2)^2}(d_L^2+d_R^2)+\frac{2}{\hat{t}(\hat{s}-m_Z^2)}d_L+\frac{1}{\hat{t}^2}\right) \\ &-\frac{c_{WWW}}{\gamma^2}\frac{\hat{s}}{\Lambda^2}\left(\frac{3}{4\gamma^2}\frac{\hat{s}^2}{(\hat{s}-m_Z^2)^2}(d_L^2+d_R^2)-3\frac{\hat{t}-m_W^2}{\hat{t}}\frac{\hat{s}}{\hat{s}-m_Z^2}d_L-\frac{3\hat{s}}{\hat{t}}\right)\Bigg]\end{aligned} \tag{2.11}$$

where

$$\begin{aligned}\beta^2 &= 1-4m_W^2/\hat{s} \\ \gamma^{-2} &= 4m_W^2/\hat{s} \\ d_R &= 2|Q|\frac{s^2}{c^2}\beta^2 \\ d_L &= d_R+\frac{3-4s^2}{c^2}\end{aligned}$$

$\hat{s}$, $\hat{t}$, and $\hat{u}$ are Mandelstam variables, and Q is the charge on the initial state quarks. Note that only the standard model interference term was included; the c_{WWW}^2 term was omitted as it is suppressed by a factor of Λ^4. We can see that the dimension-six term has the factor of $\hat{s}/\Lambda^2$ mentioned earlier; it is responsible for the deviation from the standard model curve at higher energies (see Figure 2.1). At sufficiently high energy, this cross section will violate the unitarity bound.

The anomalous couplings framework addresses the unitarity problem by means of form factors. The form factor approach promotes operator coefficients from constants to functions of momentum. The functions are chosen so as to reduce the influence of the operators at high energies, thus preventing a violation of unitarity [5].[1] While form factors solve the problem of unitarity violation, they are rather arbitrary, their only requirement being a falloff at high energies. Their momentum dependence also adds complexity to calculations.

In the effective field theory framework, unitarity violation is not a concern. In practice, unitarity is not violated until the energy is at least of order Λ, by which point the theory is no longer valid. The need for form factors is eliminated by the fact that an effective field theory puts an explicit limit on its own energy domain. It is important to note that one will typically be interested in an effective field theory only at energies for which there is data, in order to place bounds on operator coefficients. Since data cannot violate

[1] The momentum suppression function typically has the form $(1+s/\Lambda^2)^{-n}$, where Λ is referred to the cut-off energy and is not the same as the mass scale Λ in an effective field theory.

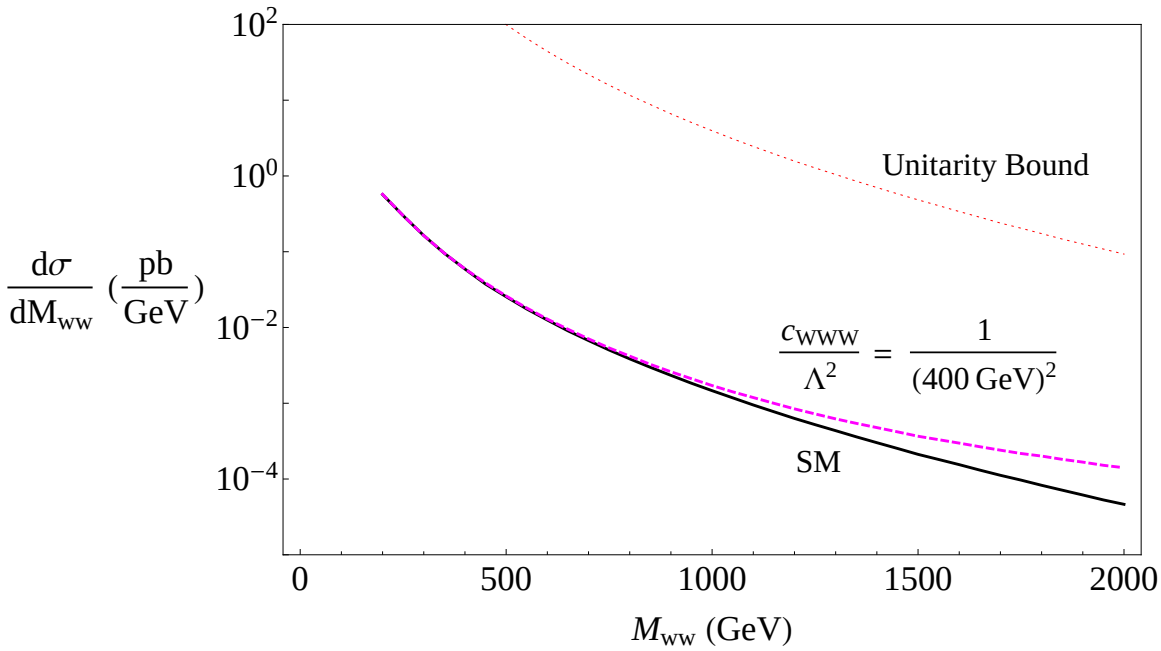

Figure 2.1: Cross section versus invariant mass for the process $pp \to W^+W^-$ at the LHC. The solid (black) curve represents the standard model result, the dashed (magenta) curve includes the dimension-six operator $\mathcal{O}_{WWW}$, and the dotted (red) curve is the unitarity bound. $\frac{c_{WWW}}{\Lambda^2}$ is set to $(400\text{ GeV})^{-2}$. Figure produced by Wolfgang Kilian with Whizard [6] and checked by the author with Madgraph [7].

unitarity by the assumptions of S-matrix theory, the effective field theory will also remain valid in the region of interest. The scale Λ will generally be far beyond the energy of available data. If the data were near the scale of new physics, there would likely be resonances associated with new particles which effective field theory is incapable of capturing. Figure 2.1 illustrates this point. For $c_{WWW} \sim 1$, the energy scale Λ has been set in the hundreds of GeV, and it is clear that the cross section does not come close to the unitarity bound even at 2 TeV. It should be noted that normally the scale Λ is assumed to be larger than this; the smaller value was used to make the deviation from the standard model curve more clear.

Chapter 3

Precision Electroweak Analysis at One Loop

In this chapter, we continue an analysis begun in Refs. [2, 8, 9] on the loop-level effects of effective operators on precision electroweak observables. Those papers focused on the divergent portions of the loop diagrams and did not appreciate that finite and unambiguous bounds could be obtained on the coefficients of the effective operators. We will use the full (finite plus divergent) expressions in order to obtain unambiguous bounds on a particular pair of effective operator coefficients. These calculations will involve only weak boson self-energy corrections, also called oblique corrections. Methods for organizing and applying such corrections to observables are well known [10, 11, 12] and will be used throughout the analysis.

3.1 A Pair of Operators

As mentioned in Section 2.1, there are five purely bosonic operators that first contribute to boson self-energy corrections at one-loop level. In Section 2.3, we bounded three of them at tree level from weak boson pair production data. This chapter will focus on the remaining two operators,

$$\mathcal{O}_{WW} = \phi^\dagger \hat{W}^{\mu\nu} \hat{W}_{\mu\nu} \phi \tag{3.1a}$$

$$\mathcal{O}_{BB} = \phi^\dagger \hat{B}^{\mu\nu} \hat{B}_{\mu\nu} \phi \tag{3.1b}$$

The above two operators affect precision electroweak observables only through oblique corrections. When the Higgs field takes its vacuum expectation value, both operators appear to affect the boson self energies at tree level; however, because the operators have the same form as the standard model gauge kinetic terms, all corrections generated by these operators that involve only gauge bosons can be absorbed into the standard model through field and coupling redefinitions. Thus, the only observable corrections from these operators arise from effective interactions involving gauge bosons and at least one Higgs or Goldstone boson. For this reason, these operators cannot be bounded from processes involving only vector bosons; however, they have been bounded previously from Higgs-mediated boson production at LEP, the Tevatron,

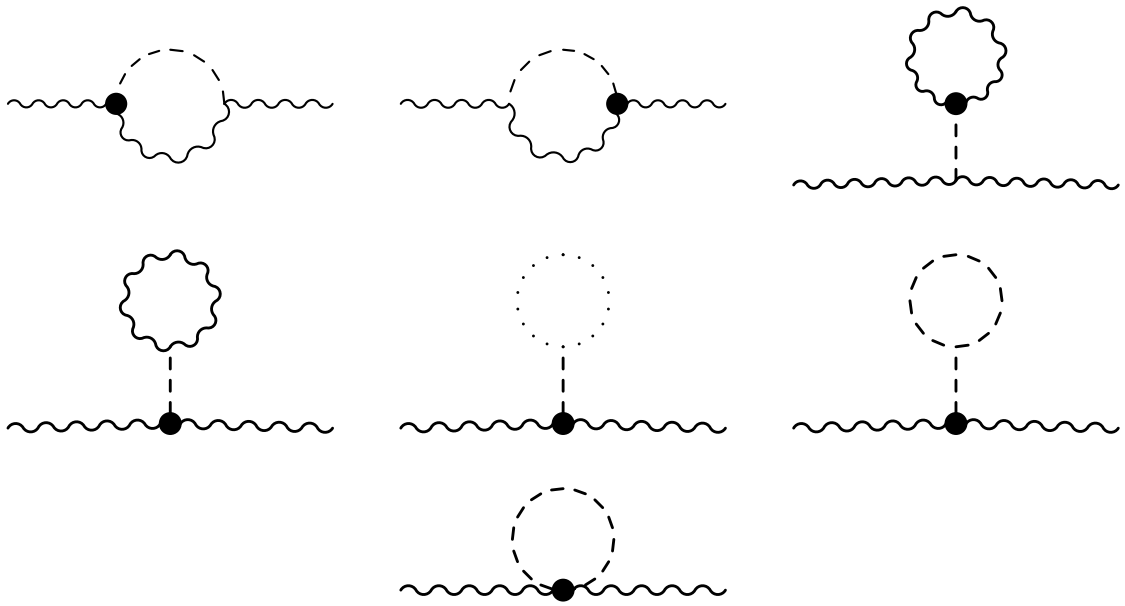

Figure 3.1: Loop-level contributions of the operators $\mathcal{O}_{WW}$ and $\mathcal{O}_{BB}$. Wavy lines represent gauge bosons, dashed lines represent Higgs or Goldstone bosons, dotted lines represent ghost fields, and the black dots represent effective operator interactions.

and the LHC [13, 14, 15, 16]. There are also papers in the literature which purport to calculate bounds from precision electroweak data [2, 17]; we address the methods in these analyses in Section 3.5.

Explicitly, the new interactions generated by the operators $\mathcal{O}_{WW}$ and $\mathcal{O}_{BB}$ that contribute at the one-loop level are

$$\begin{aligned}\mathcal{L}_{eff} = \mathcal{L}_{SM} - \frac{c_{WW}}{\Lambda^2}\frac{g^2}{8}\left(2W^+_{\mu\nu}W^{-\mu\nu} + c^2 Z_{\mu\nu}Z^{\mu\nu} + s^2 A_{\mu\nu}A^{\mu\nu} + 2scA_{\mu\nu}Z^{\mu\nu}\right) \\ \times\left(2\phi^+\phi^- + 2vH + HH + \phi^0\phi^0\right) \\ - \frac{c_{BB}}{\Lambda^2}\frac{g'^2}{8}\left(s^2 Z_{\mu\nu}Z^{\mu\nu} + c^2 A_{\mu\nu}A^{\mu\nu} - 2scA_{\mu\nu}Z^{\mu\nu}\right) \\ \times\left(2\phi^+\phi^- + 2vH + HH + \phi^0\phi^0\right)\end{aligned} \tag{3.2}$$

where s and c are the sine and cosine of the weak mixing angle. These interactions induce several corrections to the gauge boson self energies at the one-loop level. The general structure of the relevant diagrams appears in Figure 3.1, and the explicit self-energy corrections can be found in Appendix B.

The corrected self energies contain divergences that must be eliminated in order to arrive at meaningful results. Because of the gauge-invariant structure of the effective field theory, divergences arising from opera-

tors of a given dimension can always be absorbed by some other operator of the same dimension. As shown in Ref. [2], the operator

$$\mathcal{O}_{BW} = \phi^\dagger \hat{W}^{\mu\nu} \hat{B}_{\mu\nu} \phi \tag{3.3}$$

contributes to gauge boson self energies at tree level and is able to absorb all oblique divergences arising from the operators $\mathcal{O}_{WW}$ and $\mathcal{O}_{BB}$. Thus the operator $\mathcal{O}_{BW}$ must be included in our analysis.

3.2 Oblique Corrections to Precision Electroweak Observables

In this section, we will lay out the procedures for computing effective operator corrections to precision electroweak observables. Because our set of operators only affects precision electroweak observables through gauge boson propagators, it will not be necessary to calculate corrections to diagrams for every observable. Instead, we will compute corrections to each propagator once and use a general framework to correct the standard model expression for each observable.

3.2.1 The S, T, U Formalism

Before discussing the full framework for oblique corrections, we will discuss a popular approximation for oblique corrections. Though we will not ultimately be using this framework, it does give some insight into how our two operators will be constrained by experimental data.

The S, T, U formalism was first presented in Ref. [11, 12]. It applies to situations in which there are oblique corrections due to a heavy particle loop, where heavy means large relative to the Z boson mass. In this case, we can expand the propagator of this heavy particle in powers of q^2

$$\frac{1}{q^2 - M^2} = -\frac{1}{M^2}\left(1 + \frac{q^2}{M^2} + \dots\right) \tag{3.4}$$

It is clear that for large M, this expansion converges quickly. We might therefore expand the gauge boson propagators in powers of q^2 and truncate the series at first order. That gives the following approximations

$$\Pi_{\gamma\gamma}(q^2) \approx q^2 \frac{d}{dq^2}\Pi_{\gamma\gamma}(q^2)\big|_{q^2=0} \tag{3.5a}$$

$$\Pi_{\gamma Z}(q^2) \approx q^2 \frac{d}{dq^2}\Pi_{\gamma Z}(q^2)\big|_{q^2=0} \tag{3.5b}$$

$$\Pi_{ZZ}(q^2) \approx \Pi_{ZZ}(0) + q^2 \frac{d}{dq^2}\Pi_{ZZ}(q^2)\big|_{q^2=0} \tag{3.5c}$$

$$\Pi_{WW}(q^2) \approx \Pi_{WW}(0) + q^2 \frac{d}{dq^2}\Pi_{WW}(q^2)\big|_{q^2=0} \tag{3.5d}$$

where $\Pi_{\gamma\gamma}(0) = \Pi_{\gamma Z}(0) = 0$ by gauge invariance. Notice that there are six free parameters above. Because oblique corrections to electroweak observables depend on only three independent parameters (we choose α, m_Z, and s^2 here), three linear combinations of the six parameters in (3.5) will cancel out of the oblique corrections to any electroweak observable. The three linear combinations left over should be ultraviolet-finite. These combinations are called S, T, and U, and are defined as

$$\alpha S = 4sc\frac{d}{dq^2}\left[sc\Pi_{ZZ}(0) + (s^2 - c^2)\Pi_{\gamma Z}(0) - sc\Pi_{\gamma\gamma}(0)\right] \tag{3.6a}$$

$$\alpha T = \frac{1}{m_W^2}\left[\Pi_{WW}(0) - c^2\Pi_{ZZ}(0) - 2sc\Pi_{\gamma Z}(0) - s^2\Pi_{\gamma\gamma}(0)\right] \tag{3.6b}$$

$$\alpha U = 4s^2\frac{d}{dq^2}\left[\Pi_{WW}(0) - c^2\Pi_{ZZ}(0) - 2sc\Pi_{\gamma Z}(0) - s^2\Pi_{\gamma\gamma}(0)\right] \tag{3.6c}$$

At this point, we might consider looking up the values of S, T, and U, and bounding our effective coefficients off of these quantities. However, because the heaviest particle that will appear in a loop is the Higgs boson, our assumption of heavy particle loops is not valid here. To bound our operator coefficients from these parameters alone would be to ignore all higher-order q^2 dependence of our corrections. That does not mean, however, that the S, T, U formalism cannot tell us anything.

It turns out that $\mathcal{O}_{WW}$ contributes to both S and U, but $\mathcal{O}_{BB}$ contributes to S only.[1] Since c_{WW} is constrained by two independent quantities in this approximation, and c_{BB} is only constrained by one, we would expect the former to be more tightly constrained. Indeed, this is what we will find.

3.2.2 The Star Formalism

The star formalism, laid out in [10, 12], is a powerful framework for applying oblique corrections to electroweak observables. The idea is that oblique corrections can be absorbed completely in a redefinition of parameters in standard model amplitudes. More specifically, neutral- and charged-current amplitudes can be written at tree-level as

$$\mathcal{M}_{NC} = e_*^2\frac{QQ'}{q^2} + \frac{e_*^2}{s_*^2c_*^2}\left(I_3 - s_*^2Q\right)\frac{Z_{Z*}}{q^2 - m_{Z*}^2}\left(I_3' - s_*^2Q'\right) \tag{3.7}$$

$$\mathcal{M}_{CC} = \frac{e_*^2}{2s_*^2}I_+\frac{Z_{W*}}{q^2 - m_{W*}^2}I_- \tag{3.8}$$

where the parameters e, s, c, m_Z, and m_W, have been replaced by starred versions, and the parameters Z_{Z*} and Z_{W*} have been added to the Z and W propagators, respectively. These compact expressions represent the full set of oblique corrections to any electroweak process in the standard model. In the remainder of this

[1] Because T is a measure of custodial symmetry violation, it does not pick up a contribution from either operator.

section, we will find expressions for each of these starred quantities in terms of standard model parameters.

By inserting the corresponding oblique correction into charged- and neutral-current tree-level amplitudes, we find that the starred parameters are equal to

$$m^2_{W*}(q^2) = (1 - Z_W)q^2 + Z_W \left(m^2_{W0} + \Pi_{WW}(q^2)\right) \tag{3.9}$$

$$m^2_{Z*}(q^2) = (1 - Z_Z)q^2 + Z_Z \left(m^2_{Z0} + \Pi_{ZZ}(q^2)\right) \tag{3.10}$$

$$Z_{W*}(q^2) = 1 + \frac{d}{dq^2}\Pi_{WW}(q^2)\big|_{q^2=m^2_W} - \Pi'_{\gamma\gamma}(q^2) - \frac{c}{s}\Pi'_{\gamma Z}(q^2) \tag{3.11}$$

$$Z_{Z*}(q^2) = 1 + \frac{d}{dq^2}\Pi_{ZZ}(q^2)\big|_{q^2=m^2_Z} - \Pi'_{\gamma\gamma}(q^2) - \frac{c^2 - s^2}{sc}\Pi'_{\gamma Z}(q^2) \tag{3.12}$$

$$s^2_*(q^2) = s^2_0 - sc\Pi'_{\gamma Z}(q^2) \tag{3.13}$$

$$e^2_*(q^2) = e^2_0 + e^2\Pi'_{\gamma\gamma}(q^2) \tag{3.14}$$

$$\alpha_*(q^2) = \alpha_0 \left(1 + \Pi'_{\gamma\gamma}(q^2)\right) \tag{3.15}$$

where $\Pi'_{XY}(q^2) = (\Pi_{XY}(q^2) - \Pi_{XY}(0))/q^2$, $Z_W = 1 + \frac{d}{dq^2}\Pi_{WW}(q^2)\big|_{q^2=m^2_W}$, and $Z_Z = 1 + \frac{d}{dq^2}\Pi_{ZZ}(q^2)\big|_{q^2=m^2_Z}$. A subscript of 0 denotes the standard model quantity, without any corrections. Note that we do not put a subscript on parameters appearing as coefficients of the Π_{XY}, as any difference in the subscripted quantity would be a Λ^{-2} effect, resulting in a Λ^{-4} effect when combined with Π_{XY}. Because we are only working to order Λ^{-2}, we omit such terms.

Now we have the starred quantities in terms of standard model quantities, but we would like to eliminate the latter in favor of measured quantities. We will start with m^2_Z. Because m^2_Z is defined to be the pole of the propagator at $q^2 = m^2_Z$, we have the relation

$$m^2_{Z*}(m^2_Z) = m^2_Z \tag{3.16}$$

Substituting this into equation (3.10), we find

$$m^2_{Z0} = m^2_Z - \Pi_{ZZ}(m^2_Z) \tag{3.17}$$

Substituting into (3.10) again, we arrive at

$$m^2_{Z*}(q^2) = m^2_Z - \Pi_{ZZ}(m^2_Z) + \Pi_{ZZ}(q^2) - (q^2 - m^2_Z)\frac{d}{dq^2}\Pi_{ZZ}(q^2)\big|_{q^2=m^2_Z} \tag{3.18}$$

The next expression we will need is α_*. First, we know that α is most accurately known at $q^2 = 0$, so

$$\alpha_*(0) = \alpha \tag{3.19}$$

This gives us

$$\alpha = \alpha_0 \left(1 + \Pi'_{\gamma\gamma}(0)\right) \tag{3.20}$$

Substituting back in to (3.15),

$$\alpha_*(q^2) = \alpha \left(1 + \Pi'_{\gamma\gamma}(q^2) - \Pi'_{\gamma\gamma}(0)\right) \tag{3.21}$$

The final expression we must compute is s^2_*. This is a little more difficult because the weak mixing angle is not directly observable. We will need to make use of its tree-level expression in terms of measurable parameters. We have

$$\begin{aligned} s_0^2 &= \frac{1}{2}\left(1 - \sqrt{1 - \frac{4\pi\alpha_0}{\sqrt{2}G_{F0}m_{Z0}^2}}\right) \\ &= s^2\left[1 - \frac{c^2}{c^2 - s^2}\left(\Pi'_{\gamma\gamma}(0) + \frac{1}{m_W^2}\Pi_{WW}(0) - \frac{1}{m_Z^2}\Pi_{ZZ}(m_Z^2)\right)\right] \end{aligned} \tag{3.22}$$

where in the second line, we used equations (3.17) and (3.20), as well as the relation

$$G_F = G_{F0}\left(1 - \frac{\Pi_{WW}(0)}{m_W^2}\right) \tag{3.23}$$

Now substituting back into (3.13),

$$s_*^2 = s^2\left[1 - \frac{c}{s}\Pi'_{\gamma Z}(q^2) - \frac{c^2}{c^2 - s^2}\left(\Pi'_{\gamma\gamma}(0) + \frac{1}{m_W^2}\Pi_{WW}(0) - \frac{1}{m_Z^2}\Pi_{ZZ}(m_Z^2)\right)\right] \tag{3.24}$$

We have now arrived at expressions for all of the relevant starred quantities (we will not need m^2_{W*}). All oblique corrections to precision electroweak observables can be included by substituting in the starred versions of the variables α, m_Z, and s^2. Because of the presence of Z_{Z*} and Z_{W*} in the neutral- and charged-current amplitudes, respectively, the correction to α depends upon the type of vertex; these corrections will be labeled α_γ, α_Z, or α_W, depending on the mediating boson. The full set of starred quantities for energies

at the Z-pole or higher is

$$\alpha_{\gamma *} \to \alpha \left(1 + \Pi'_{\gamma\gamma}(q^2) - \Pi'_{\gamma\gamma}(0)\right) \tag{3.25a}$$

$$\begin{aligned}\alpha_{Z *} \to \alpha &\left(1 + \Pi'_{\gamma\gamma}(q^2) - \Pi'_{\gamma\gamma}(0)\right) \\ &\times \left(1 + \frac{d}{dq^2}\Pi_{ZZ}(q^2)\big|_{q^2=m_Z^2} - \Pi'_{\gamma\gamma}(q^2) - \frac{c^2 - s^2}{cs}\Pi'_{\gamma Z}(q^2)\right)\end{aligned} \tag{3.25b}$$

$$\begin{aligned}\alpha_{W *} \to \alpha &\left(1 + \Pi'_{\gamma\gamma}(q^2) - \Pi'_{\gamma\gamma}(0)\right) \\ &\times \left(1 + \frac{d}{dq^2}\Pi_{WW}(q^2)\big|_{q^2=m_W^2} - \Pi'_{\gamma\gamma}(q^2) - \frac{c}{s}\Pi'_{\gamma Z}(q^2)\right)\end{aligned} \tag{3.25c}$$

$$m_{Z *}^2 \to m_Z^2 - \Pi_{ZZ}(m_Z^2) + \Pi_{ZZ}(q^2) - (q^2 - m_Z^2)\frac{d}{dq^2}\Pi_{ZZ}(q^2)\big|_{q^2=m_Z^2} \tag{3.25d}$$

$$s_*^2 \to s^2\left[1 - \frac{c}{s}\Pi'_{\gamma Z}(q^2) - \frac{c^2}{c^2 - s^2}\left(\Pi'_{\gamma\gamma}(0) + \frac{1}{m_W^2}\Pi_{WW}(0) - \frac{1}{m_Z^2}\Pi_{ZZ}(m_Z^2)\right)\right] \tag{3.25e}$$

The correction to any electroweak observable X measured at an energy at or above the Z-pole is given by

$$\delta X = \frac{\delta X}{\delta \alpha}\delta\alpha + \frac{\delta X}{\delta m_Z^2}\delta m_Z^2 + \frac{\delta X}{\delta s^2}\delta s^2 \tag{3.26}$$

where $\delta p = p_* - p$ for each parameter p.

We mentioned that the above expressions are for measurements taken at Z-pole energies or above. At low energies ($q \approx 0$), we can rewrite the matrix elements in terms of the Fermi constant

$$\mathcal{M}_{NC} = -4\sqrt{2}G_F\rho_*(0)\left(I_3 - s_*^2(0)Q\right)\left(I_3' - s_*^2(0)Q'\right) \tag{3.27}$$

$$\mathcal{M}_{CC} = -2\sqrt{2}G_F I_+ I_- \tag{3.28}$$

where the $\rho_*(0)$ factor comes from the combination of equations (3.17) and (3.23) and is equal to

$$\rho_*(0) = \frac{1 + \frac{1}{m_W^2}\Pi_{WW}(0)}{1 + \frac{1}{m_Z^2}\Pi_{ZZ}(0)} \approx 1 + \frac{1}{m_W^2}\Pi_{WW}(0) - \frac{1}{m_Z^2}\Pi_{ZZ}(0) \tag{3.29}$$

Thus, low-energy observables are affected by corrections to s^2 and by corrections to ρ

$$\delta X = \frac{\delta X}{\delta s^2}\delta s^2 + \frac{\delta X}{\delta \rho}\delta\rho \tag{3.30}$$

where $\delta\rho = \rho_*(0) - 1$. The standard model value of ρ is unity.

	Notation	Measurement
Z-pole	Γ_Z	Total Z width
	$\sigma_{\rm had}$	Hadronic cross section
	$R_f(f=e,\mu,\tau,b,c)$	Ratios of decay rates
	$A_{FB}^{0,f}(f=e,\mu,\tau,b,c,s)$	Forward-backward asymmetry
	$\bar{s}_l^2$	Hadronic charge asymmetry
	$A_f(f=e,\mu,\tau,b,c,s)$	Polarized asymmetries
Fermion pair production at LEP2	$\sigma_f(f=q,e,\mu,\tau)$	Total cross sections for $e^+e^-\to f\bar{f}$
	$A_{FB}^f(f=\mu,\tau)$	Forward-backward asymmetries for $e^+e^-\to f\bar{f}$
W mass and decay rate	m_W	W mass from LEP and Tevatron
	Γ_W	W width from Tevatron
DIS and atomic parity violation	$Q_W(Cs)$	Weak charge in Cs
	$Q_W(Tl)$	Weak charge in Tl
	$Q_W(e)$	Weak charge of the electron
	g_L^2, g_R^2	ν_μ-nucleon scattering from NuTeV
	$g_V^{\nu e}, g_A^{\nu e}$	ν-e scattering from CHARM II

Table 3.1: Precision electroweak quantities. Data taken from [4, 18, 19].

3.3 Summary of Precision Electroweak Observables

A list of the observables included in this analysis can be found in Table 3.1. The observables can be divided into four different categories, based on how they are measured. Z-pole observables are measured from $e^+e^-\to ff$ at LEP1 and the SLC. Fermion pair production cross sections and forward-backward asymmetries were measured at LEP2 at several energies ranging from 130 GeV to 207 GeV. The W mass and width were measured at the Tevatron and LEP2. The remaining observables were calculated from a variety of low-energy deep inelastic scattering and atomic parity violation experiments. Each observable will be defined in the following subsections.

3.3.1 Z-pole Observables

All Z-pole observables are measured at the Z mass and can be derived from the partial decay widths and polarized asymmetries for each fermion. The standard model expressions are

$$\Gamma_{ff} = \frac{\alpha m_Z}{12 s^2 c^2}\left({g_V^f}^2 + {g_A^f}^2\right) \tag{3.31}$$

$$A_f = \frac{2 g_V^f g_A^f}{{g_V^f}^2 + {g_A^f}^2} \tag{3.32}$$

where g_V^f and g_A^f are

f	g_V^f	g_A^f
ν_e, ν_μ, ν_τ	$+\frac{1}{2}$	$+\frac{1}{2}$
e, μ, τ	$-\frac{1}{2} + 2s^2$	$-\frac{1}{2}$
u, c, t	$+\frac{1}{2} - \frac{4}{3}s^2$	$+\frac{1}{2}$
d, s, b	$-\frac{1}{2} + \frac{2}{3}s^2$	$-\frac{1}{2}$

The standard model expressions for the Z-pole observables are

$$\Gamma_Z = \sum_f \Gamma_{ff} \tag{3.33}$$

$$\sigma_h^0 = \frac{12\pi}{m_Z^2} \frac{\Gamma_{ee}\Gamma_{had}}{\Gamma_Z^2} \tag{3.34}$$

$$R_f = \begin{cases} \frac{\Gamma_{had}}{\Gamma_{ff}} & \text{for } f = e, \mu, \tau \\ \frac{\Gamma_{ff}}{\Gamma_{had}} & \text{for } f = b, c \end{cases} \tag{3.35}$$

$$A_{FB}^{0,f} = \frac{3}{4} A_e A_f, \qquad f = e, \mu, \tau, b, c, s \tag{3.36}$$

$$\bar{s}_l^2 = s^2 \tag{3.37}$$

$$A_f, \qquad f = e, \mu, \tau, b, c, s \tag{3.38}$$

3.3.2 Fermion Pair Production Cross Sections

Fermion production cross sections were measured at twelve different energies at LEP2, an e^+e^- collider. The standard model expressions can be determined from the appropriate Feynman diagrams (see Figure 3.2). For production of quarks, muons, and tau leptons, the only diagrams are s-channel diagrams mediated by a Z or photon. The amplitude for these diagrams is

$$\begin{aligned} \mathcal{M} = &\frac{4\pi\alpha}{\hat{s} - m_Z^2 + i\Gamma_Z m_Z} \frac{1}{4c^2 s^2} \bar{v}(p')\gamma^\mu \left(g_V^e - g_A^e \gamma^5\right) u(p) \bar{u}(k)\gamma_\mu \left(g_V^f - g_A^f \gamma^5\right) v(k') \\ &- \frac{4\pi\alpha Q_f}{\hat{s}} \bar{v}(p')\gamma^\mu u(p)\bar{u}(k)\gamma_\mu v(k') \end{aligned} \tag{3.39}$$

where p, p' are the momenta of the incoming electron-positron pair and k, k' are the outgoing fermion momenta. $\hat{s}$ is the square of the total momentum, $(p + p')^2 = (k + k')^2$.

For production of electron-positron pairs, t-channel diagrams are also possible. The complete amplitude

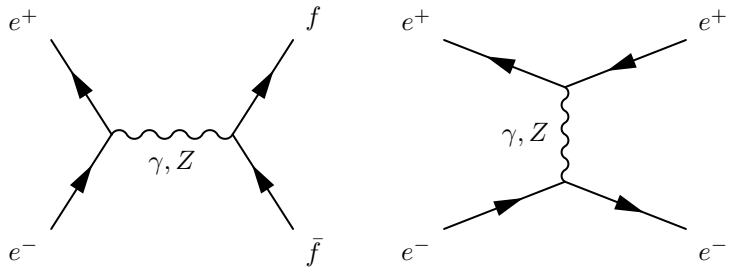

Figure 3.2: The s- (*left*) and t-channel (*right*) diagrams for fermion pair production. The t-channel diagram only applies to electron-positron production.

for e^+e^- production is

$$\begin{aligned}\mathcal{M} = &\frac{4\pi\alpha}{\hat{s} - m_Z^2 + i\Gamma_Z m_Z}\frac{1}{4c^2s^2}\bar{v}(p')\gamma^\mu\left(g_V^e - g_A^e\gamma^5\right)u(p)\bar{u}(k)\gamma_\mu\left(g_V^f - g_A^f\gamma^5\right)v(k') \\ &- \frac{4\pi\alpha}{\hat{t} - m_Z^2 + i\Gamma_Z m_Z}\frac{1}{4c^2s^2}\bar{u}(k)\gamma^\mu\left(g_V^e - g_A^e\gamma^5\right)u(p)\bar{v}(p')\gamma_\mu\left(g_V^e - g_A^e\gamma^5\right)v(k') \\ &+ \frac{4\pi\alpha}{\hat{s}}\bar{v}(p')\gamma^\mu u(p)\bar{u}(k)\gamma_\mu v(k') - \frac{4\pi\alpha}{\hat{t}}\bar{u}(k)\gamma^\mu u(p)\bar{v}(p')\gamma_\mu v(k')\end{aligned} \tag{3.40}$$

where $\hat{t}$ is defined as $(p-k)^2 = (p'-k')^2$.

3.3.3 W mass and width

The W mass correction can be derived from its standard model expression. Here a 0 subscript will denote uncorrected standard model quantities. We have

$$m_{W0}^2 = \frac{4\pi\alpha_0}{s_0^2}\frac{1}{4\sqrt{2}G_{F0}} \tag{3.41}$$

Using equations (3.22) and (3.23), and combining with the relation $m_W^2 = m_{W0}^2 + \Pi_{WW}(m_W^2)$, we arrive at

$$\delta m_W^2 = \Pi_{WW}(m_W^2) + \frac{s^2}{c^2 - s^2}\Pi_{WW}(0) - \frac{c^4}{c^2 - s^2}\Pi_{ZZ}(m_Z^2) + \frac{s^2}{c^2 - s^2}m_W^2\Pi'_{\gamma\gamma}(0) \tag{3.42}$$

The W width is defined by

$$\Gamma_W = \frac{3\alpha m_W}{4s^2} \tag{3.43}$$

Equation (3.26) can be used to determine oblique corrections (note that because $m_{W*}^2(m_W^2) = m_W^2$, we needn't compute a deviation for that parameter.

3.3.4 Low-Energy Observables

These experiments are performed at energies far below the W mass, so we assume $q^2 = 0$ for the corresponding observables. Recall that for these observables, we use equation (3.30) to determine the dimension-six corrections. Note also that $\rho(0) = 1$.

Weak charges of atoms are measured in atomic parity violation experiments. The weak charge of an atom with Z protons and N neutrons is given by

$$Q_W(Z,N) = -2\left[(2Z+N)C_{1u} + (Z+2N)C_{1d}\right] \tag{3.44}$$

where $C_{1u} = 2\rho g_A^e g_V^u$ and $C_{1d} = 2\rho g_A^e g_V^d$.

The weak charge of the electron is measured in Møller scattering. The expression is

$$Q_W(e) = -2C_{2e} = -4\rho g_A^e g_V^e \tag{3.45}$$

Effective couplings for neutrino-nucleon scattering were measured at NuTeV. Their expressions are

$$g_L^2 = g_{L,eff}^{u2} + g_{L,eff}^{d2} \tag{3.46}$$

$$g_R^2 = g_{R,eff}^{u2} + g_{R,eff}^{d2} \tag{3.47}$$

$$\tag{3.48}$$

The quantities on the right hand sides of the above expressions are effective couplings between Z bosons and up and down quarks. These are completely distinct from the dimension-six operator couplings treated in this dissertation. The expressions for these couplings are

$$g_{L,eff}^{u2} = \rho\frac{g_V^u + g_A^u}{2} \tag{3.49}$$

$$g_{R,eff}^{u2} = \rho\frac{g_V^u - g_A^u}{2} \tag{3.50}$$

$$g_{L,eff}^{d2} = \rho\frac{g_V^d + g_A^d}{2} \tag{3.51}$$

$$g_{R,eff}^{d2} = \rho\frac{g_V^d - g_A^d}{2} \tag{3.52}$$

$$\tag{3.53}$$

Effective couplings for neutrino-electron scattering were measured at CHARM II. Their expressions are

$$g_V^{\nu e} = \rho g_V^e \tag{3.54}$$

$$g_A^{\nu e} = \rho g_A^e \tag{3.55}$$

3.4 Bounds on Effective Operator Coefficients

We now apply equations (3.26) and (3.30) to the electroweak observables of Section 3.3. In order to obtain a bound on the coefficients c_{WW}/Λ^2 and c_{BB}/Λ^2, we use the χ^2 statistic

$$\chi^2 = \sum_{i,j} \chi^i \left(\sigma^{-1}\right)_{ij} \chi^j \tag{3.56}$$

where $\chi^i = \left(X^i_{SM} - X^i_{exp} + \frac{c_{WW}}{\Lambda^2} X^i_{WW} + \frac{c_{BB}}{\Lambda^2} X^i_{BB} + \frac{c_{BW}}{\Lambda^2} X^i_{BW}\right)$, X^i_j being the correction of operator $\mathcal{O}_j$ to the i^{th} observable. σ_{ij} is the error matrix, related to the errors for each observable, σ_i, and the error correlation matrix, ρ_{ij} [4, 19],

$$\sigma_{ij} = \sigma_i \rho_{ij} \sigma_j \tag{3.57}$$

We calculate the bounds by first setting c_{BW} to the value (as a function of c_{WW} and c_{BB}) which minimizes χ^2. We then write this new χ^2 in the following way

$$\chi^2\big|_{c_{BW}=c_{BW}^{min}} = \chi^2_{min} + \frac{\sum_{ij}(c_i - \hat{c}_i) M_{ij} (c_j - \hat{c}_j)}{\Lambda^4} \qquad i,j \in \{WW, BB\} \tag{3.58}$$

where χ^2_{min} is the value of χ^2 minimized with respect to all coefficients, $\hat{c}_i$ is the best fit value of the coefficient c_i, and M_{ij} is a symmetric matrix. We arrive at bounds by solving the equation

$$\frac{\sum_{ij}(c_i - \hat{c}_i) M_{ij} (c_j - \hat{c}_j)}{\Lambda^4} = 1 \tag{3.59}$$

We can diagonalize M_{ij} to find two statistically independent combinations of our two operators and obtain a bound on those. We find

$$\begin{pmatrix} 0.999 & 0.0385 \\ -0.0385 & 0.999 \end{pmatrix} \times \frac{1}{\Lambda^2} \begin{pmatrix} c_{WW} \\ c_{BB} \end{pmatrix} = \begin{pmatrix} 129.4 \pm 120.7 \text{ TeV}^{-2} \\ -482.3 \pm 3160 \text{ TeV}^{-2} \end{pmatrix} \tag{3.60}$$

The contributions of the two coefficients are essentially decoupled due to the fact that the net effect of $\mathcal{O}_{WW}$ is significantly larger than that of $\mathcal{O}_{BB}$. While both coefficients are consistent with zero at 2σ, the central value of $\mathcal{O}_{WW}$ differs from zero by just over one standard deviation. These bounds are considerably weaker than bounds from Higgs-mediated boson production [13, 14, 15, 16], which have uncertainties on the order of 10 TeV^{-2}.

If we instead compute bounds for each coefficient separately, setting the other coefficient to zero in each case, we obtain

$$\frac{c_{WW}}{\Lambda^2} = 129.5 \pm 120.8 \text{ TeV}^{-2} \tag{3.61a}$$

$$\frac{c_{BB}}{\Lambda^2} = 1456 \pm 2225 \text{ TeV}^{-2} \tag{3.61b}$$

We again see that $\mathcal{O}_{WW}$ is significantly more tightly constrained than $\mathcal{O}_{BB}$.

3.5 Comparison to Previous Studies

This marks the first time bounds have been obtained using the full power of the effective field theory framework. There are other papers which compute bounds on the electroweak effective operator coefficients, including the operators $\mathcal{O}_{WW}$ and $\mathcal{O}_{BB}$ [2, 17]; however, those analyses differ from ours in a few important respects.

First, as stated explicitly in Ref. [2], those papers make the substitution

$$\frac{1}{\epsilon} - \gamma + \ln(4\pi\mu^2) + 1 \to \ln \Lambda^2 \tag{3.62}$$

This is equivalent to setting the renormalization scale to Λ. Because precision electroweak data is taken at energies around the Z-pole, the scale should be set to m_Z. At scale Λ, loop amplitudes have terms that go like $\ln \frac{m_Z^2}{\Lambda^2}$, so that perturbation theory breaks down at sufficiently large Λ. As an example, running the S parameter to 1 TeV using the renormalization group equations gives an answer 10% smaller than Refs. [2, 17] get by setting the renormalization scale to Λ directly [20]. This difference grows to 20% at 10 TeV. In Section 3.6, we will discuss this topic further.

Another difference in previous analyses is that only divergent terms (and a few terms which grow at least logarithmically with m_h) were used to calculate operator bounds. This approximation is unnecessary and is inaccurate unless Λ is much larger than m_Z. More signficantly, because all divergent terms can be absorbed by tree-level operators, the loop-level coefficients will only appear in linear combinations defined

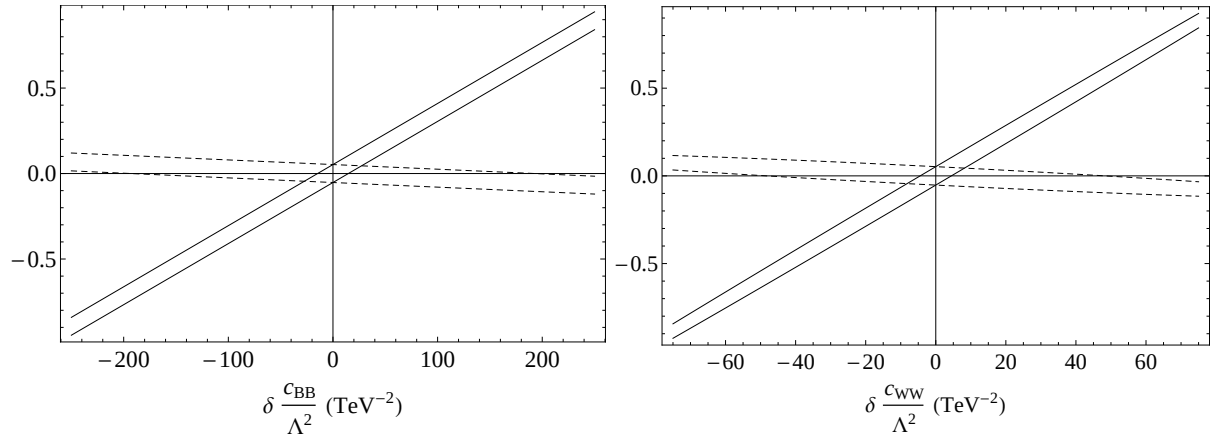

Figure 3.3: One-sigma uncertainty regions in c_{BB}/Λ^2 and c_{WW}/Λ^2. The vertical axis is the deviation in c_{BW}/Λ^2. Regions are given for renormalization scale $\mu = m_Z$ (dashed line) and $\mu = \Lambda = 1$ TeV (solid line).

by the renormalized tree-level coefficients. This makes it impossible to put bounds on both c_{WW} and c_{BB} simultaneously, since the divergences of $\mathcal{O}_{WW}$ and $\mathcal{O}_{BB}$ are absorbed into c_{BW} and therefore always appear in the same linear combination. Our analysis, on the other hand, includes all finite terms, breaking this redundancy and allowing the calculation of global bounds.

The final, and most significant, difference is that previous analyses allowed only one operator coefficient to be non-zero at a time. Because tree-level operators such as $\mathcal{O}_{BW}$ are necessary for absorbing divergences, setting them to zero requires a fine-tuning which sets their finite contributions to zero. There is no reason for such a fine-tuning to occur. These previous results thus contain misleadingly strong bounds on loop-level operators. The plots in Figure 3.3 illustrate that setting the renormalization scale to a higher value and fixing the tree-level coefficient c_{BW} significantly strengthen the loop-level operator bounds. These tighter bounds are misleading; the coefficient c_{BW} should be allowed to "float," that is, to assume whatever value minimizes χ^2. This is necessary to arrive at a result independent of renormalization scale.

3.6 Renormalization Group Evolution

As discussed earlier, the bounds obtained in Section 3.4 are independent of renormalization scale. Allowing the coefficient c_{BW} to float allows that parameter to compensate for any shift in renormalization scale, keeping the coefficients c_{WW} and c_{BB} constant. If, however, we were to include higher-order corrections, the renormalization scale would reappear; it is not as though we have rendered the scale irrelevant. In fact, we might ask what our bounds would look like had we taken data at some other energy. Because most of our data is taken at energies around the Z mass, it is natural to consider $\mu = m_Z$ to be our renormalization scale. In this section we will use renormalization group equations (RGEs) to evolve our bounds up from m_Z

up to energies where we might expect to find new physics.

The relevant RGE for the evolution of our operators is

$$\mu\frac{d}{d\mu}\begin{bmatrix} c_{BB} \\ c_{WW} \\ c_{BW} \end{bmatrix} = \gamma_{BW}\begin{bmatrix} c_{BB} \\ c_{WW} \\ c_{BW} \end{bmatrix} \tag{3.63}$$

where γ_{BW} is the anomalous dimension matrix for the three operators.

The following solution to the above RGE follows Ref. [20]. The anomalous dimension matrix is given by

$$\gamma_{BW} = \frac{1}{16\pi^2}\begin{pmatrix} \frac{1}{2}g_1^2 - \frac{9}{2}g_2^2 + 12\lambda + 2Y & 0 & 3g_2^2 \\ 0 & -\frac{3}{2}g_1^2 - \frac{5}{2}g_2^2 + 12\lambda + 2Y & g_1^2 \\ 2g_1^2 & 2g_2^2 & -\frac{1}{2}g_1^2 + \frac{9}{2}g_2^2 + 4\lambda + 2Y \end{pmatrix} \tag{3.64}$$

where Y is a function of the quark and lepton Yukawa matrices

$$Y = \mathrm{Tr}\left(3Y_u^\dagger Y_u + 3Y_d^\dagger Y_d + Y_e^\dagger Y_e\right) \approx 3y_t^2 \tag{3.65}$$

In order to evaluate the RGE, we can rewrite the anomalous dimension matrix

$$\mu\frac{d}{d\mu}\begin{bmatrix} c_{BB} \\ c_{WW} \\ c_{BW} \end{bmatrix} = \left(\gamma_{BW}\big|_{Y=0} + \frac{3y_t^2}{8\pi^2}\, I\right)\begin{bmatrix} c_{BB} \\ c_{WW} \\ c_{BW} \end{bmatrix} \tag{3.66}$$

where I is the identity matrix.

Now define a function $r(\mu)$ such that

$$\mu\frac{d}{d\mu}r(\mu) = \frac{3y_t^2}{8\pi^2}r(\mu) \tag{3.67}$$

The function $r(\mu)$ can be computed numerically. We can now give an approximate solution to the RGE in terms of $r(\mu)$

$$\begin{bmatrix} c_{BB}(\mu) \\ c_{WW}(\mu) \\ c_{BW}(\mu) \end{bmatrix} = \frac{r(\mu)}{r(m_Z)}\left(1 - \gamma_{BW}\big|_{Y=0}\log\frac{m_Z}{\mu}\right)\begin{bmatrix} c_{BB}(m_Z) \\ c_{WW}(m_Z) \\ c_{BW}(m_Z) \end{bmatrix} \tag{3.68}$$

This expression is accurate to within a few percent up to several TeV.

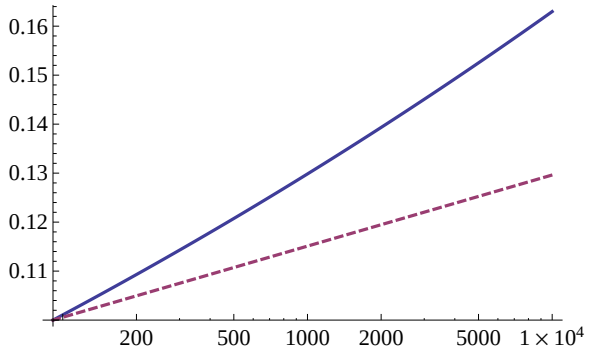

Figure 3.4: Evolution of the effective coefficient $c_{BW}(\mu)$. The solid (blue) line is the renormalization group evolution; the dashed (purple) line is the result of simply setting the renormalization scale to Λ. For the renormalization group evolution, coefficients were set at Z-pole values of ($c^0_{BW} = 0.1, c^0_{WW} = 1, c^0_{BB} = 2$).

If we use the above expression to run the coefficient c_{BW} from m_Z to Λ, we get

$$c_{BW}(\Lambda) = \frac{r(\Lambda)}{r(m_Z)}\left[c_{BW}(m_Z)\left(1 - \frac{\left(\frac{s^2}{c^2}\frac{g^2}{2} - \frac{9g^2}{2} - 4\lambda\right)\log\frac{\Lambda}{m_Z}}{16\pi^2}\right) + \frac{g^2}{8\pi^2}\left(c_{WW}(m_Z) + \frac{s^2}{c^2}c_{BB}(m_Z)\right)\log\frac{\Lambda}{m_Z}\right] \tag{3.69}$$

Compare this to the relation found in Ref. [2], derived by simply setting the renormalization scale to Λ:

$$c_{BW}(m_h) = c_{BW}(\Lambda) - \frac{g^2}{8\pi^2}\left(c_{WW}(\Lambda) + \frac{s^2}{c^2}c_{BB}(\Lambda)\right)\log\frac{\Lambda}{m_h} \tag{3.70}$$

If we invert this relation and change the scale from m_h to m_Z, we arrive at

$$c_{BW}(\Lambda) = c_{BW}(m_Z) + \frac{g^2}{8\pi^2}\left(c_{WW}(m_Z) + \frac{s^2}{c^2}c_{BB}(m_Z)\right)\log\frac{\Lambda}{m_h} \tag{3.71}$$

Comparing equations (3.69) and (3.71), we notice that the latter result leaves out the $r(\mu)$ function entirely and is missing a correction to the $c_{BW}(m_Z)$ contribution. At $\Lambda = 3$ TeV, $r(\Lambda)/r(m_Z)$ is about 14% if $r(m_Z)$ is normalized to unity, and the correction to $c_{BW}(m_Z)$ is about 5%, so it is clear that the difference is non-negligible.

Because we have determined bounds on c_i/Λ^2, and here we are only evolving the c_i, it does not make sense to plot the evolution as a function of Λ using the bounds we computed. However, for the sake of illustration, Figure 3.4 shows the evolution of c_{BW} using relations (3.69) and (3.71), given an arbitrary set of values of c_{WW}, c_{BB}, and c_{BW} at the Z-pole. The difference between the two relations at large Λ is quite significant.

3.7 Conclusions

Using the effective field theory framework, we have obtained bounds at one-loop level on the dimension-six operator coefficients $\frac{c_{WW}}{\Lambda^2}$ and $\frac{c_{BB}}{\Lambda^2}$ using precision electroweak data. Because the loop diagrams of Figure 3.1 contain ultraviolet divergences, the operator $\mathcal{O}_{BW}$ was included to absorb them. By allowing the coefficient c_{BW} to float, we were able to obtain bounds which are independent of renormalization scale. Our procedure was shown to be more accurate and complete than similar analyses in the literature. Finally, we showed that the effective field theory framework allows us to evolve our coefficients to higher energy scales using the renormalization group. Though the bounds presented in this chapter are looser than those taken from Higgs-mediated boson production at high-energy colliders, this analysis is an important illustration of the proper use of the effective field theory framework.

Chapter 4

Global Analysis of Electroweak Operators

In the previous chapter, we computed bounds on the two loop-level electroweak operators $\mathcal{O}_{BB}$ and $\mathcal{O}_{WW}$ from precision electroweak data. In this chapter, we will extend our analysis to the full set of operators in equation (2.2). We will continue to use the framework introduced in Chapter 3, now including diagrams from all five loop-level operators. We will need to include all four tree-level operators from equation (2.1) in order to absorb divergences. We will also need to make minor changes to our procedure to account for vertex corrections.

4.1 Contributions from Loop-Level Operators

The set of operators which affects precision electroweak observables at one loop can be found in equation (2.2). These five operators affect both gauge boson self energies and vertices. Table 4.1 lists the contribution of each operator to each self energy and vertex diagrammatically. Explicit expressions for all self energy and vertex corrections can be found in Appendix B.

4.1.1 Vertex Corrections

Note that although our operators do not contain fermion interactions, there are still loop-level corrections to the fermion-fermion-boson vertices. This would seem to pose a problem for our analysis, as the framework we introduced in Chapter 3 is only valid for oblique corrections. The solution is to absorb vertex corrections into the oblique corrections.

Consider the corrections to a 2-to-2 charged-current process in the presence of a dimension-six operator. There are four diagrams:

$\mathcal{M}$ =

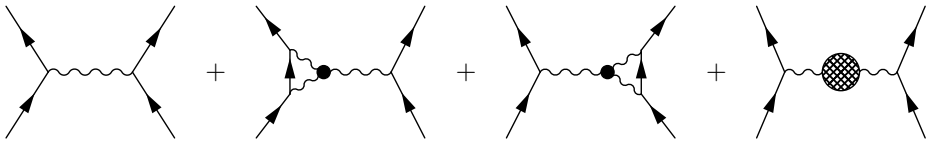

(4.1)

where the small black dots represent dimension-six TGCs, and the large cross-hatched circle represents tree- or loop-level corrections to the W self energy. If we label the above diagrams $\mathcal{M}_1$ through $\mathcal{M}_4$, then the expressions for each amplitude are

$$\mathcal{M}_1 = \left(\frac{g}{\sqrt{2}}\right)^2 \left[\bar{v}\gamma_\mu \frac{1}{2}\left(1-\gamma^5\right) u\right] \frac{g^{\mu\nu} - q^\mu q^\nu/q^2}{q^2 - m_W^2} \left[\bar{u}\gamma_\nu \frac{1}{2}\left(1-\gamma^5\right) v\right] \tag{4.2a}$$

$$\mathcal{M}_2 = \frac{g}{\sqrt{2}} \left[\bar{v}\Delta\Gamma^W_\mu u\right] \frac{g^{\mu\nu} - q^\mu q^\nu/q^2}{q^2 - m_W^2} \left[\bar{u}\gamma_\nu \frac{1}{2}\left(1-\gamma^5\right) v\right] \tag{4.2b}$$

$$\mathcal{M}_3 = \frac{g}{\sqrt{2}} \left[\bar{v}\gamma_\mu \frac{1}{2}\left(1-\gamma^5\right) u\right] \frac{g^{\mu\nu} - q^\mu q^\nu/q^2}{q^2 - m_W^2} \left[\bar{u}\Delta\Gamma^W_\nu v\right] \tag{4.2c}$$

$$\mathcal{M}_4 = \left(\frac{g}{\sqrt{2}}\right)^2 \left[\bar{v}\gamma_\mu \frac{1}{2}\left(1-\gamma^5\right) u\right] \frac{g^{\mu\alpha} - q^\mu q^\alpha/q^2}{q^2 - m_W^2} \Delta\Pi^{WW}_{\alpha\beta} \frac{g^{\beta\nu} - q^\beta q^\nu/q^2}{q^2 - m_W^2} \left[\bar{u}\gamma_\nu \frac{1}{2}\left(1-\gamma^5\right) v\right] \tag{4.2d}$$

Now if we make the following definitions

$$\Delta\Gamma^W_\mu \equiv \frac{g}{\sqrt{2}}\gamma_\mu \frac{1}{2}\left(1-\gamma^5\right)\Delta\Gamma^W \tag{4.3}$$

$$\Delta\Pi^{WW}_{\mu\nu} \equiv g_{\mu\nu}\Delta\Pi^{WW}_T \tag{4.4}$$

we can see that

$$\mathcal{M}_2 = \mathcal{M}_3 = \mathcal{M}_1 \Delta\Gamma^W \tag{4.5}$$

$$\mathcal{M}_4 = \mathcal{M}_1 \Delta\Pi^{WW}_T \frac{1}{q^2 - m_W^2} \tag{4.6}$$

and so the cross section is proportional to

$$\sigma_{CC} \propto |\mathcal{M}|^2 = |\mathcal{M}_1 + \mathcal{M}_2 + \mathcal{M}_3 + \mathcal{M}_4|^2 \tag{4.7}$$

$$= |\mathcal{M}_1|^2 \left|1 + 2\Delta\Gamma^W + \Delta\Pi^{WW}_T \frac{1}{q^2 - m_W^2}\right|^2 \tag{4.8}$$

Thus, we see that charged-current processes will only depend on the linear combination[1]

$$\Delta\overline{\Pi}^{WW}_T \equiv \Delta\Pi^{WW}_T + 2(q^2 - m_W^2)\Delta\Gamma^W \tag{4.9a}$$

Neutral-current interactions are a bit more complicated because of interference between photon- and Z-

[1] Note that there is a sign difference between our equation (4.9a) and equation (4.6) of Ref. [2] due to differing sign conventions. The difference does not affect corrections to observables.

mediated diagrams, but similar relations exist for those self energies as well

$$\Delta\overline{\Pi}_T^{\gamma\gamma} \equiv \Delta\Pi_T^{\gamma\gamma} + 2sq^2\Delta\Gamma^{\gamma} \tag{4.9b}$$

$$\Delta\overline{\Pi}_T^{\gamma Z} \equiv \Delta\Pi_T^{\gamma Z} + sq^2\Delta\Gamma^{Z} + c(q^2 - m_Z^2)\Delta\Gamma^{\gamma} \tag{4.9c}$$

$$\Delta\overline{\Pi}_T^{ZZ} \equiv \Delta\Pi_T^{ZZ} + 2c(q^2 - m_Z^2)\Delta\Gamma^{Z} \tag{4.9d}$$

Here we have made the substitution $\Delta\Gamma_\mu^V \equiv gT_3^f\gamma_\mu\frac{1}{2}\left(1-\gamma^5\right)\Delta\Gamma^V$, where T_3^f is the third isospin component of the fermions in the vertex. This factor comes about because of the antisymmetry of the W bosons in the vertex loop. The vertex correction is independent of fermion charge. The modified self energies above allow us to fold all vertex corrections into the self energy corrections and reuse the formalism adopted in Chapter 3.

4.1.2 Checks on Self Energy Corrections

The vertex and self-energy corrections in this analysis were computed using the FeynCalc package [21] for Mathematica, which produces expressions for loop integrals in terms of scalar integral functions. The LoopTools [22] package was used to numerically evaluate the scalar integrals. To ensure that these expressions were accurate, several checks were used.

R_ξ Gauge

Because the choice of gauge is arbitrary, all observable consequences of a gauge theory must be gauge-independent. All of the loop calculations in this dissertation were done in the R_ξ gauge, which is a parametrization of all possible gauge choices. The gauge parameter ξ must cancel out of all observable quantities; in fact, it cancels out of each operator's contribution to each modified self energy. While a gauge-invariant result does not verify the accuracy of gauge-independent diagrams, it is useful for fixing multiplicative factors and relative signs between gauge-dependent diagram contributions.

Because calculations were performed in the R_ξ gauge, all fields, physical and non-physical, had to be included in diagrams. This is in contrast to the popular unitary gauge, in which non-physical fields such as ghosts and Goldstone bosons are zeroed out. The parameter ξ appears in gauge boson propagators in addition to ghost and Goldstone mass terms; this makes R_ξ gauge useful for checking diagrams with gauge boson loops.

Comparison with Literature Despite the notable shortcomings of Ref. [2] and others (discussed in Chapter 3), their results can be used as a partial check on the expressions in the present analysis. In particular,

Appendix B of [2] lists the divergent contributions of every operator to each modified self energy. The divergences are written in terms of a cutoff, while our analysis used the gauge-invariant method of dimensional regularization, but it is straightforward to compare the two.

By-Hand Calculations For all operators except for $\mathcal{O}_W$ and $\mathcal{O}_B$, I computed the contribution of all loop diagrams by hand. These were done using dimensional regularization in R_ξ gauge. These expressions were compared with the numerical results from Feyncalc and LoopTools. An example computation, the contribution to the W self energy by $\mathcal{O}_{BB}$, appears below

$$\begin{aligned}
i\Pi^{BB}_{WW}(q^2) &= \frac{1}{2}\frac{c_{BB}}{\Lambda^2}\frac{ig^2v}{2}(2ivs_W^2)\frac{i}{-m_h^2}\left[p^\alpha(-p)^\beta + p^2 g^{\alpha\beta}\right]\frac{-i}{p^2-m_Z^2}\left[g_{\alpha\beta} - \frac{p_\alpha p_\beta}{p^2-\xi m_Z^2}(1-\xi)\right] \\
&= \frac{1}{2}\frac{c_{BB}}{\Lambda^2}\frac{g^2v^2s_W^2}{m_h^2}\int\frac{d^dp}{(2\pi)^d}\frac{(d-1)p^2}{p^2-m_Z^2} \\
&= i\frac{1}{2}\frac{c_{BB}}{\Lambda^2}\frac{g^2v^2s_W^2}{m_h^2}\frac{d(d-1)}{2(4\pi)^{d/2}}\Gamma\left[-\frac{d}{2}\right]m_Z^d \\
&= -i\frac{1}{2}\frac{c_{BB}}{\Lambda^2}g^2v^2s_W^2\frac{m_Z^d}{m_h^2}\frac{d-1}{(4\pi)^{d/2}}\Gamma\left[1-\frac{d}{2}\right] \\
&= i\frac{1}{2}\frac{c_{BB}}{\Lambda^2}g^2v^2s_W^2\frac{m_Z^4}{m_h^2}\frac{3}{16\pi^2}\left(\frac{1}{\epsilon}-\gamma+\ln 4\pi-\ln\mu^2-\ln\frac{m_Z^2}{\mu^2}+\frac{1}{3}\right) \\
&= i\frac{c_{BB}}{\Lambda^2}2c_W^2s_W^2\frac{m_Z^6}{m_h^2}\frac{3}{16\pi^2}\left(\frac{1}{\epsilon}-\gamma+\ln 4\pi-\ln\mu^2-\ln\frac{m_Z^2}{\mu^2}+\frac{1}{3}\right)
\end{aligned}$$

Notice that the ξ dependence drops out. Here we use the $\overline{\text{MS}}$ scheme, meaning that we drop the terms $\frac{1}{\epsilon}-\gamma+\ln 4\pi-\ln\mu^2$.

4.2 Renormalization of Tree-Level Operators

In Chapter 3, we needed only the operator $\mathcal{O}_{BW}$ to absorb the divergences of the two loop-level operators. The addition of three additional loop-level operators necessitates the inclusion of the remaining three tree-level operators of equation (2.1). In this section, we will show explicitly that all divergences can be removed by a suitable renormalization of the coefficients c_{BW}, $c_\phi^{(3)}$, c_{DW}, and c_{DB}. By considering divergent plus tree-level contributions to the starred parameters of Section 3.2.2, we can solve for renormalized tree-level quantities in terms of loop-level coefficients.

Because the parameter $\rho_*(0)$ violates custodial symmetry, it only receives tree-level corrections from the custodial-symmetry-violating operator $\mathcal{O}_\phi^{(3)}$. We can therefore use its divergent part to find an expression

for $c_\phi^{(3)r}$, the renormalized coefficient. The divergent plus tree-level contributions to $\rho_*(0)$ are

$$\rho_*^{div}(0) = \frac{c_{\phi,1}}{\Lambda^2}\frac{v^2}{2} - \frac{3g^2s^2}{64\pi^2c^2\Lambda^2}\left((m_h^2+3m_W^2)c_B + 3m_W^2c_W\right)E \tag{4.10}$$

where E represents the divergent portion of the contribution. We can see that the renormalized coefficient must be

$$c_{\phi,1}^r = c_{\phi,1} + \frac{3g^2s^2}{32\pi^2v^2c^2}\left((m_h^2+3m_W^2)c_B + 3m_W^2c_W\right)E \tag{4.11}$$

We can use a similar procedure for the remaining operators. The expressions for $\alpha_{\gamma*}$ and m_{Z*}^2 only involve c_{DW} and c_{DB}

$$\alpha_{\gamma*}^{div} = \frac{2g^2s^2}{\Lambda^2}q^2(c_{DB}+c_{DW}) + \frac{g^2s^2}{96\pi^2\Lambda^2}q^2(c_B+c_W) \tag{4.12}$$

$$m_{Z*}^2 = \frac{2g^2s^4}{c^3\Lambda^2}(m_W^2-c^2q^2)^2\left(c_{DB}+\frac{c_B}{192\pi^2}E\right) + \frac{2g^2}{c^2\Lambda^2}(m_W^2-c^2q^2)^2\left(c_{DW}+\frac{c_W}{192\pi^2}E\right) \tag{4.13}$$

This uniquely defines c_{DB}^r and c_{DW}^r.

Finally, using our other expressions and the divergent plus tree-level portion of Z_{W*}, we can find c_{BW}^r. The expression for Z_{W*}^{div} is

$$\begin{aligned} Z_{W*}^{div} = {} & \frac{c_{BW}}{\Lambda^2}m_W^2 + 2\frac{c_{DW}}{\Lambda^2}g^2(2m_W^2-q^2) - \frac{1}{16\pi^2}\left(\frac{3}{2}\frac{c_{WWW}}{\Lambda^2}g^4m_W^2 - \frac{s^2}{c^2}\frac{c_{BB}}{\Lambda^2}g^2m_W^2 - \frac{c_{WW}}{\Lambda^2}g^2m_W^2\right. \\ & \left. + \frac{1}{24c^2}\frac{c_B}{\Lambda^2}g^2(4c^2m_h^2+(7+20c^2)m_W^2) + \frac{1}{24c^2}\frac{c_W}{\Lambda^2}g^2(3c^2m_h^2-(3+20c^2)m_W^2+4c^2q^2)\right)E \end{aligned} \tag{4.14}$$

The renormalized tree-level coefficients then are

$$c_{\phi,1}^r = c_{\phi,1} + \frac{3g^2s^2}{32\pi^2v^2c^2}\left((m_h^2+3m_W^2)c_B + 3m_W^2c_W\right)E \tag{4.15}$$

$$c_{DB}^r = c_{DB} - \frac{c_B}{192\pi^2}E \tag{4.16}$$

$$c_{DW}^r = c_{DW} - \frac{c_W}{192\pi^2}E \tag{4.17}$$

$$\begin{aligned} c_{BW}^r = {} & c_{BW} - \frac{g^2}{16\pi^2}\left(c_{WW} + \frac{s^2}{c^2}c_{BB} - \frac{3}{2}c_{WWW}g^2 - \frac{1}{24c^2m_W^2}c_B(3c^2m_h^2+(7+20c^2)m_W^2)\right. \\ & \left. - \frac{1}{24c^2m_W^2}c_W(3c^2m_h^2-(3+12c^2)m_W^2)\right)E \end{aligned} \tag{4.18}$$

We can check and verify that these definitions absorb all divergences in the observables that we didn't use in the derivations above. Because these operators absorb all ultraviolet divergences, we will be able to obtain scale-invariant bounds on the loop-level operators.

4.3 Results

4.3.1 Global Bounds on Electroweak Operators

We now take all of the self-energy corrections from Appendix B and compute oblique corrections to precision electroweak observables using the star formalism. We use the following values for input parameters

$$\alpha(m_Z) = 1/128.91, \qquad v = 246.2 \text{ GeV}, \qquad m_Z = 91.1876 \text{ GeV}, \qquad m_h = 125 \text{ GeV} \tag{4.19}$$
$$m_t = 172.9 \text{ GeV}, \qquad m_b = 4.79 \text{ GeV}, \qquad m_\tau = 1.777 \text{ GeV}$$

All other fermions are assumed to have a mass of zero.

Here we again use the χ^2 statistic to compute bounds on the operators.

$$\chi^2 = \sum_{i,j} \chi^i \left(\sigma_{ij}\right)^{-1} \chi^j \tag{4.20}$$

where σ_{ij} is the error matrix, as defined in equation (3.57), and

$$\chi^i = \left(X^i_{SM} - X^i_{exp} + \sum_k \frac{c_k}{\Lambda^2} X^i_k \right) \tag{4.21}$$

where the sum on k runs over all loop- and tree-level operators.

We will first obtain scale-dependent bounds on all operators simultaneously, followed by scale-independent bounds on the loop-level operators.

We begin by writing χ^2 in the following way

$$\chi^2 = \chi^2_{min} + \frac{\sum_{ij}(c_i - \hat{c}_i) M_{ij} (c_j - \hat{c}_j)}{\Lambda^4} \tag{4.22}$$

where the i, j sum is over all nine operators. The $\hat{c}_i$ are best-fit values. We then arrive at 1σ bounds by solving the equation

$$\frac{\sum_{ij}(c_i - \hat{c}_i) M_{ij} (c_j - \hat{c}_j)}{\Lambda^4} = 1 \tag{4.23}$$

It is cleanest to diagonalize the matrix M and present bounds on the nine linearly independent combinations

of operators. Those bounds appear below

$$\begin{pmatrix} -0.000 & -0.001 & 0.000 & -0.000 & -0.000 & -0.164 & 0.986 & -0.018 & 0.025 \\ -0.000 & -0.002 & 0.001 & 0.000 & -0.000 & -0.494 & -0.103 & -0.832 & -0.230 \\ 0.000 & -0.001 & 0.001 & -0.001 & -0.000 & -0.838 & -0.131 & 0.527 & -0.051 \\ -0.001 & -0.000 & 0.002 & 0.000 & 0.000 & -0.165 & -0.006 & -0.170 & 0.972 \\ -0.913 & -0.218 & 0.145 & -0.312 & 0.011 & 0.001 & -0.000 & 0.001 & -0.001 \\ -0.156 & 0.961 & 0.184 & -0.129 & 0.031 & -0.002 & 0.000 & -0.001 & -0.001 \\ 0.099 & 0.066 & -0.727 & -0.675 & -0.030 & -0.001 & 0.000 & -0.001 & 0.002 \\ -0.361 & 0.150 & -0.645 & 0.653 & 0.062 & -0.002 & -0.000 & 0.000 & 0.001 \\ 0.040 & -0.035 & 0.011 & -0.053 & 0.997 & -0.000 & 0.000 & 0.000 & -0.000 \end{pmatrix} \tag{4.24}$$

$$\times \frac{1}{\Lambda^2} \begin{pmatrix} c_{WWW} \\ c_W \\ c_B \\ c_{WW} \\ c_{BB} \\ c_{BW} \\ c_{\phi,1} \\ c_{DW} \\ c_{DB} \end{pmatrix} = \begin{pmatrix} -0.004 & \pm & 0.010 \\ 0.062 & \pm & 0.086 \\ 0.022 & \pm & 0.143 \\ 0.628 & \pm & 0.387 \\ -149.2 & \pm & 120.9 \\ -17.7 & \pm & 187.5 \\ 589.3 & \pm & 455.1 \\ -3715 & \pm & 1904 \\ 3902 & \pm & 9964 \end{pmatrix} \text{ TeV}^{-2} \tag{4.25}$$

Note that the tree-level and loop-level bounds are essentially decoupled from each other. The first four bounds represent bounds on linear combinations of tree-level operators and are very tightly constrained. The final five are bounds on linear combinations of loop-level operators. These bounds are weaker than the tree-level bounds by three orders of magnitude or more. Most of these bounds are consistent with zero at 1σ, but a few differ by more. The bound on c_{DB} (fourth row) is only consistent with zero at 1.6σ. Among loop-level operators, the bound on c_{WWW} (fifth row) is consistent with zero at 1.2σ, and bounds on the two linear combinations of c_B and c_{WW} (seventh and eighth rows) are consistent with zero at 1.3σ and 1.95σ. These loop-level bounds are still far too weak to speculate about the presence of any new physics.

We can calculate scale-independent bounds by first setting the tree-level operators to the values (as a function of the loop-level operators) which minimize χ^2. We again write this new χ^2 in matrix form

$$\chi^2\big|_{\{c_{tree}\}=\{c_{tree}^{min}\}} = \chi^2_{min} + \frac{\sum_{ij}(c_i - \hat{c}_i)M_{ij}(c_j - \hat{c}_j)}{\Lambda^4} \tag{4.26}$$

where $\{c_{tree}\}$ is the set of all tree-level operators, and the sum on i, j runs over all loop-level operators. We then follow the same procedure as before to arrive at bounds on the loop-level operators

$$\begin{pmatrix} -0.913 & -0.218 & 0.145 & -0.312 & 0.011 \\ -0.156 & 0.961 & 0.184 & -0.129 & 0.031 \\ -0.099 & -0.066 & 0.727 & 0.675 & 0.030 \\ 0.361 & -0.150 & 0.645 & -0.653 & -0.062 \\ 0.040 & -0.035 & 0.011 & -0.053 & 0.997 \end{pmatrix} \times \frac{1}{\Lambda^2} \begin{pmatrix} c_{WWW} \\ c_W \\ c_B \\ c_{WW} \\ c_{BB} \end{pmatrix} = \begin{pmatrix} -149.2 & \pm & 120.9 \\ -17.7 & \pm & 187.5 \\ 589.3 & \pm & 455.1 \\ -3715 & \pm & 1904 \\ 3902 & \pm & 9964 \end{pmatrix} \text{ TeV}^{-2} \quad (4.27)$$

Notice that these bounds are identical to the bounds above, highlighting the fact that the two sets of operators are decoupled in the eigenvector matrix.

4.3.2 Interpretation of Bounds

The results presented in Section 4.3.1 are one-sigma bounds on linear combinations of effective operator coefficients divided by the mass scale Λ squared. Thus, the bounds are really on two independent quantities. It is reasonable to ask whether we can infer any sort of bound on either the bare coefficients or the scale Λ. While we cannot make any such inference with any certainty, there are a few things we can say.

Firstly, if we want the new physics to be perturbative (i.e. not strongly coupled), we can put an approximate upper bound on the c_i. Roughly, if c_i is the magnitude of the coupling between the standard model and new physics, then at tree level, we will have an amplitude proportional to c_i. Then, at one loop, we will pick up another vertex, plus a loop factor, so that our loop amplitude is proportional to $c_i^2/(4\pi)^2$. If we want our theory to be perturbative, we must have

$$c_i > \frac{c_i^2}{(4\pi)^2} \quad (4.28)$$

$$\Rightarrow c_i < (4\pi)^2 \quad (4.29)$$

This provides a rough upper bound for the c_i. On the low end, unless there is suppression due to some symmetry, we would expect c_i to be at least order unity, especially since we have included factors of the coupling constants in the operator definitions. These two constraints together give a rough idea of what our bounds say about the scale Λ, subject to the assumptions above. With this in mind, the bounds of equation 4.27 are not strong enough to rule out new physics at the TeV scale.

4.3.3 Final Thoughts

In this chapter, I have presented a global analysis of electroweak sector effective operators. I obtained bounds on the full set of nine operators, as well as scale-independent bounds on the five loop-level operators. The tree-level operators are well-constrained, as is well-documented in the literature [2, 17]. Bounds on the loop-level operators are rather weak compared with tree-level bounds from high-energy collider experiments, which produce bounds one to two orders of magnitude tighter in the case of c_W, c_B, and c_{WWW} (see Chapter 2, and three orders of magnitude tighter in the case of c_{WW} and c_{BB} [15, 16]. Though this analysis did not yield the best available bounds on loop-level operators, it is important as a complete demonstration of the use of effective field theory in loop calculations.

Because the strongest bounds are derived from high-energy data, one would expect constraints on effective operators to become significantly stronger as more data is collected from the LHC. Loop analyses such as the one performed in this dissertation may be valuable for constraining operators which don't contribute to collider data at tree-level, such as Higgs-sector operators.

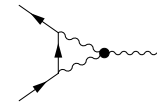	Γ_W Γ_Z Γ_γ	$\mathcal{O}_{WWW}$, $\mathcal{O}_B$, $\mathcal{O}_W$ $\mathcal{O}_{WWW}$, $\mathcal{O}_B$, $\mathcal{O}_W$ $\mathcal{O}_{WWW}$, $\mathcal{O}_B$, $\mathcal{O}_W$
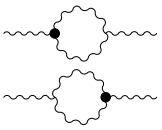	Π_{WW} Π_{ZZ} $\Pi_{\gamma\gamma}$ $\Pi_{\gamma Z}$	$\mathcal{O}_{WWW}$, $\mathcal{O}_B$, $\mathcal{O}_W$ $\mathcal{O}_{WWW}$, $\mathcal{O}_B$, $\mathcal{O}_W$ $\mathcal{O}_{WWW}$, $\mathcal{O}_B$, $\mathcal{O}_W$ $\mathcal{O}_{WWW}$, $\mathcal{O}_B$, $\mathcal{O}_W$
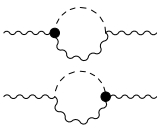	Π_{WW} Π_{ZZ} $\Pi_{\gamma\gamma}$ $\Pi_{\gamma Z}$	$\mathcal{O}_B$, $\mathcal{O}_W$, $\mathcal{O}_{WW}$ $\mathcal{O}_B$, $\mathcal{O}_W$, $\mathcal{O}_{BB}$, $\mathcal{O}_{WW}$ $\mathcal{O}_B$, $\mathcal{O}_W$ $\mathcal{O}_B$, $\mathcal{O}_W$, $\mathcal{O}^*_{BB}$, $\mathcal{O}^*_{WW}$ $*$ top diagram only
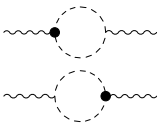	Π_{WW} Π_{ZZ} $\Pi_{\gamma\gamma}$ $\Pi_{\gamma Z}$	$\mathcal{O}_W$ $\mathcal{O}_B$, $\mathcal{O}_W$ $\mathcal{O}_B$, $\mathcal{O}_W$ $\mathcal{O}_B$, $\mathcal{O}_W$
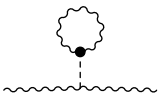	Π_{WW} Π_{ZZ} $\Pi_{\gamma\gamma}$ $\Pi_{\gamma Z}$	$\mathcal{O}_{BB}$, $\mathcal{O}_{WW}$ $\mathcal{O}_{BB}$, $\mathcal{O}_{WW}$
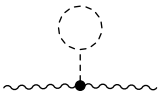	Π_{WW} Π_{ZZ} $\Pi_{\gamma\gamma}$ $\Pi_{\gamma Z}$	$\mathcal{O}_{WW}$ $\mathcal{O}_{BB}$, $\mathcal{O}_{WW}$ $\mathcal{O}_{BB}$, $\mathcal{O}_{WW}$ $\mathcal{O}_{BB}$, $\mathcal{O}_{WW}$
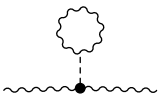	Π_{WW} Π_{ZZ} $\Pi_{\gamma\gamma}$ $\Pi_{\gamma Z}$	$\mathcal{O}_{WW}$ $\mathcal{O}_{BB}$, $\mathcal{O}_{WW}$ $\mathcal{O}_{BB}$, $\mathcal{O}_{WW}$ $\mathcal{O}_{BB}$, $\mathcal{O}_{WW}$
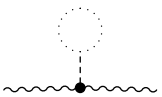	Π_{WW} Π_{ZZ} $\Pi_{\gamma\gamma}$ $\Pi_{\gamma Z}$	$\mathcal{O}_{WW}$ $\mathcal{O}_{BB}$, $\mathcal{O}_{WW}$ $\mathcal{O}_{BB}$, $\mathcal{O}_{WW}$ $\mathcal{O}_{BB}$, $\mathcal{O}_{WW}$
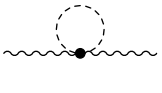	Π_{WW} Π_{ZZ} $\Pi_{\gamma\gamma}$ $\Pi_{\gamma Z}$	$\mathcal{O}_{WW}$ $\mathcal{O}_{BB}$, $\mathcal{O}_{WW}$ $\mathcal{O}_{BB}$, $\mathcal{O}_{WW}$ $\mathcal{O}_{BB}$, $\mathcal{O}_{WW}$
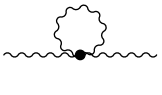	Π_{WW} Π_{ZZ} $\Pi_{\gamma\gamma}$ $\Pi_{\gamma Z}$	$\mathcal{O}_W$ $\mathcal{O}_W$ $\mathcal{O}_W$

Table 4.1: Contributions of each loop-level operator to boson self-energy and vertex corrections by diagram.

Appendix A

Unitarity Bound Derivation

We start with the partial wave expansion for a scattering amplitude T:

$$T(\lambda_1\lambda_2 \to \lambda_3\lambda_4) = 16\pi \sum_{j=0}^{\infty} (2j+1) a_j D^j_{\lambda_1-\lambda_2,\lambda_3-\lambda_4} \tag{A.1}$$

Note that the D-functions are orthogonal:

$$\int d(\cos\theta) D^j_{\lambda_1-\lambda_2,\lambda_3-\lambda_4} D^{j'\,*}_{\lambda_1-\lambda_2,\lambda_3-\lambda_4} = \frac{2}{2j+1}\delta^{jj'} \tag{A.2}$$

Thus

$$\int d(\cos\theta)|T|^2 = 2|N|^2 \sum_{j=0}^{\infty}(2j+1)|a_j|^2 \tag{A.3}$$

Define the scattering amplitude in terms of the S matrix, $S = 1 + iT$. Unitarity requires that

$$T^\dagger T = 2\mathrm{Im}(T) \tag{A.4}$$

Now take the matrix element of (A.4) between identical two-body states and insert a complete set of intermediate states on the left-hand side. This can then be written as

$$\int dPS_2\, |T^{el}|^2 + \sum_n \int dPS_n\, |T^{in}|^2 = 2\,\mathrm{Im}(T^{el}) \tag{A.5}$$

$$\int dPS_2\, |T^{el}|^2 + \sum_{\lambda_3,\lambda_4} \int dPS_2\, |T^{in}|^2 \leq 2\,\mathrm{Im}(T^{el}) \tag{A.6}$$

where we removed the sum over n and selected a single 2-body inelastic scattering process. For massless

elastic-scattering particles, the phase space integral gives

$$\frac{1}{16\pi}\int d(\cos\theta)\,|T^{el}|^2 + \sum_{\lambda_3,\lambda_4}\int dPS_2\,|T^{in}|^2 \le 2\,\mathrm{Im}(T^{el}) \tag{A.7}$$

$$\sum_{j=0}^{\infty}(2j+1)|a_j^{el}|^2 + \frac{1}{32\pi}\sum_{\lambda_3,\lambda_4}\int dPS_2\,|T^{in}|^2 \le \sum_{j=0}^{\infty}(2j+1)\mathrm{Im}(a_j^{el}) \tag{A.8}$$

Now we will assume that the elastic process is dominated by the $j = 1$ mode and throw away all other terms:

$$3|a_0^{el}|^2 + \frac{1}{32\pi}\sum_{\lambda_3,\lambda_4}\int dPS_2\,|T^{in}|^2 \le 3\mathrm{Im}(a_0^{el}) \tag{A.9}$$

$$\frac{1}{32\pi}\sum_{\lambda_3,\lambda_4}\int dPS_2\,|T^{in}|^2 \le 3\mathrm{Im}(a_0^{el})\left(1-\mathrm{Im}(a_0^{el})\right) \tag{A.10}$$

$$\frac{1}{32\pi}\sum_{\lambda_3,\lambda_4}\int dPS_2\,|T^{in}|^2 \le \frac{3}{4} \tag{A.11}$$

$$\sum_{\lambda_3,\lambda_4}\int dPS_2\,|T^{in}|^2 \le 24\pi \tag{A.12}$$

For the process $q\bar{q} \to WW$, averaging over colors and initial-state spins, we find the bound

$$\sigma_{tot} = \frac{1}{2\hat{s}}\frac{1}{9}\sum_{colors}\frac{1}{4}\sum_{\lambda_1,\lambda_2}\sum_{\lambda_3,\lambda_4}\int dPS_2\,|T^{in}|^2 \tag{A.13}$$

$$\le \frac{2\pi}{\hat{s}} \tag{A.14}$$

Appendix B

Self Energy Corrections

B.1 Tree-Level Contributions

$$\Delta\Pi_{WW} = -\frac{c_{DW}}{\Lambda^2}2g^2q^4 \tag{B.1}$$

$$\Delta\Pi_{ZZ} = -\frac{c_{BW}}{\Lambda^2}2m_W^2s^2q^2 + \frac{c_{\phi,1}}{\Lambda^2}\frac{v^2}{2}m_Z^2 - \frac{c_{DW}}{\Lambda^2}2g^2c^2q^4 - \frac{c_{DB}}{\Lambda^2}2g^2\frac{s^4}{c^2}q^4 \tag{B.2}$$

$$\Delta\Pi_{\gamma\gamma} = \frac{c_{BW}}{\Lambda^2}2m_W^2s^2q^2 - \frac{c_{DW}}{\Lambda^2}2g^2s^2q^4 - \frac{c_{DB}}{\Lambda^2}2g^2s^2q^4 \tag{B.3}$$

$$\Delta\Pi_{\gamma Z} = \frac{c_{BW}}{\Lambda^2}m_W^2\frac{s}{c}(c^2-s^2)q^2 - \frac{c_{DW}}{\Lambda^2}2g^2scq^4 + \frac{c_{DB}}{\Lambda^2}2g^2\frac{s^3}{c}q^4 \tag{B.4}$$

B.2 Loop-Level Contributions

$\mathcal{O}_{BB}$:

$$\Delta\Pi_{WW} = \frac{c_{BB}}{\Lambda^2}\frac{1}{16\pi^2}\frac{g^2m_Z^4s^4}{m_h^2}\left(2m_Z^2 - 3A_0\left(m_Z^2\right)\right) \tag{B.5}$$

$$\begin{aligned}\Delta\Pi_{ZZ} = \frac{c_{BB}}{\Lambda^2}\frac{1}{16\pi^2}\frac{g^2s^4}{m_h^2c^2}\Big[&2m_h^2m_Z^2\left(q^2 - m_h^2 + m_Z^2\right)B_0\left(q^2, m_h^2, m_Z^2\right)\\ &- m_Z^2\left(3q^2 + 2m_h^2 + 3m_Z^2\right)A_0\left(m_Z^2\right) + m_h^2\left(2m_Z^2 - q^2\right)A_0\left(m_h^2\right)\\ &-6m_W^2q^2A_0\left(m_W^2\right) + 4m_W^4q^2 + 2m_Z^4q^2 + 2m_Z^6\Big]\end{aligned} \tag{B.6}$$

$$\begin{aligned}\Delta\Pi_{\gamma\gamma} = -\frac{c_{BB}}{\Lambda^2}\frac{1}{16\pi^2}\frac{g^2q^2s^2}{m_h^2}\Big[&m_h^2A_0\left(m_h^2\right) + 3m_Z^2A_0\left(m_Z^2\right)\\ &+6m_W^2A_0\left(m_W^2\right) - 4m_W^4 - 2m_Z^4\Big]\end{aligned} \tag{B.7}$$

$$\begin{aligned}\Delta\Pi_{\gamma Z} = \frac{c_{BB}}{\Lambda^2}\frac{1}{16\pi^2}\frac{g^2s^3}{m_h^2c}\Big[&m_h^2m_Z^2\left(m_h^2 - m_Z^2 - q^2\right)B_0\left(q^2, m_h^2, m_Z^2\right)\\ &+ m_Z^2\left(m_h^2 + 3q^2\right)A_0\left(m_Z^2\right) - m_h^2\left(m_Z^2 - q^2\right)A_0\left(m_h^2\right)\\ &+6m_W^2q^2A_0\left(m_W^2\right) - 4m_W^4q^2 - 2m_Z^4q^2\Big]\end{aligned} \tag{B.8}$$

$\mathcal{O}_{WW}$:

$$\begin{aligned}
\Delta\Pi_{WW} &= \frac{c_{WW}}{\Lambda^2}\frac{1}{16\pi^2}\frac{g^2}{m_h^2}\left[2m_h^2m_W^2\left(q^2-m_h^2+m_W^2\right)B_0\left(q^2,m_h^2,m_W^2\right)\right. \qquad \text{(B.9)}\\
&\quad -2m_W^2\left(3q^2+m_h^2+3m_W^2\right)A_0\left(m_W^2\right)+m_h^2\left(2m_W^2-q^2\right)A_0\left(m_h^2\right)\\
&\quad \left.-3\left(m_W^4+m_Z^2q^2\right)A_0\left(m_Z^2\right)+4m_W^4q^2+2m_Z^4q^2+4m_W^6+2m_W^4m_Z^2\right]\\
\Delta\Pi_{ZZ} &= \frac{c_{WW}}{\Lambda^2}\frac{1}{16\pi^2}\frac{g^2c^2}{m_h^2}\left[2m_h^2m_Z^2\left(q^2-m_h^2+m_Z^2\right)B_0\left(q^2,m_h^2,m_Z^2\right)\right. \qquad \text{(B.10)}\\
&\quad -m_Z^2\left(3q^2+2m_h^2+3m_Z^2\right)A_0\left(m_Z^2\right)+m_h^2\left(2m_Z^2-q^2\right)A_0\left(m_h^2\right)\\
&\quad \left.-6\left(m_Z^4+m_W^2q^2\right)A_0\left(m_W^2\right)+4m_W^4q^2+2m_Z^4q^2+4m_W^2m_Z^4+2m_Z^6\right]\\
\Delta\Pi_{\gamma\gamma} &= -\frac{c_{WW}}{\Lambda^2}\frac{1}{16\pi^2}\frac{g^2q^2s^2}{m_h^2}\left[m_h^2A_0\left(m_h^2\right)+3m_Z^2A_0\left(m_Z^2\right)\right. \qquad \text{(B.11)}\\
&\quad \left.+6m_W^2A_0\left(m_W^2\right)-4m_W^4-2m_Z^4\right]\\
\Delta\Pi_{\gamma Z} &= -\frac{c_{WW}}{\Lambda^2}\frac{1}{16\pi^2}\frac{g^2sc}{m_h^2}\left[m_h^2m_Z^2\left(m_h^2-m_Z^2-q^2\right)B_0\left(q^2,m_h^2,m_Z^2\right)\right. \qquad \text{(B.12)}\\
&\quad +m_Z^2\left(m_h^2+3q^2\right)A_0\left(m_Z^2\right)-m_h^2\left(m_Z^2-q^2\right)A_0\left(m_h^2\right)\\
&\quad \left.+6m_W^2q^2A_0\left(m_W^2\right)-4m_W^4q^2-2m_Z^4q^2\right]
\end{aligned}$$

$\mathcal{O}_B$:

$$\begin{aligned}
\Delta\Pi_{WW} &= \frac{c_B}{\Lambda^2}\frac{1}{16\pi^2}\frac{g^2 m_W^2 s^2}{36q^2c^2}\left[36m_W^2(q^4-m_W^4)C_0(0,0,q^2,m_W^2,0,m_Z^2)\right. \qquad \text{(B.13)}\\
&-6c^2(m_W^2-q^2)^2B_0(q^2,0,m_W^2)+3((-2s^6+19s^4-30s^2+12)m_Z^4\\
&-2(2s^4+7s^2-7)m_Z^2q^2+(5+2c^2)q^4)B_0(q^2,m_W^2,m_Z^2)-3((1+3c^2)m_Z^2+5q^2)A_0(m_W^2)\\
&\left.+3(s^2-c^2)(m_Z^2+5m_W^2-5q^2)A_0(m_Z^2)+2q^2(3s^2m_Z^2-q^2)\right]\\
\Delta\Pi_{ZZ} &= \frac{c_B}{\Lambda^2}\frac{1}{16\pi^2}\frac{g^2 s^2}{36q^2c^2}\left[72m_W^4q^2(c^2q^2-m_W^2)C_0(0,0,q^2,m_W^2,0,m_W^2)\right. \qquad \text{(B.14)}\\
&+3(-m_Z^2(m_Z^2-m_h^2)^2+(m_Z^4-8m_h^2m_Z^2-m_h^4)q^2+(m_Z^2+2m_h^2)q^4-q^6)B_0(q^2,m_h^2,m_Z^2)\\
&+3q^2(24m_W^4+8(c^2-s^2)m_W^2q^2+(c^2-s^2)q^4)B_0(q^2,m_W^2,m_W^2)\\
&+3(m_h^2m_Z^2-m_Z^4+m_h^2q^2+q^4)A_0(m_h^2)+3(m_Z^4-m_h^2m_Z^2-(10m_Z^2+m_h^2)q^2+q^4)A_0(m_Z^2)\\
&+6q^2(-12m_W^2+(10c^2+1)q^2)A_0(m_W^2)\\
&\left.+2q^2(3m_Z^4+3m_h^2m_Z^2+(3m_h^2-2(6s^4-9s^2+2)m_Z^2)q^2-2s^2q^4)\right]\\
\Delta\Pi_{\gamma\gamma} &= -\frac{c_B}{\Lambda^2}\frac{1}{16\pi^2}\frac{g^2q^2s^2}{18}\left[36m_W^4C_0(0,0,q^2,m_W^2,0,m_W^2)\right. \qquad \text{(B.15)}\\
&\left.+3(8m_W^2+q^2)B_0(q^2,m_W^2,m_W^2)+30A_0(m_W^2)+2(q^2-6m_W^2)\right]\\
\Delta\Pi_{\gamma Z} &= \frac{c_B}{\Lambda^2}\frac{1}{16\pi^2}\frac{g^2 s}{72c}\left[72m_W^4(m_W^2+(s^2-c^2)q^2)C_0(0,0,q^2,m_W^2,0,m_W^2)\right. \qquad \text{(B.16)}\\
&+3(m_h^4+4m_h^2m_Z^2-5m_Z^4-(2m_h^2-4m_Z^2)q^2+q^4)B_0(q^2,m_h^2,m_Z^2)\\
&-3(24m_W^4+8(c^2-3s^2)m_W^2q^2+(c^2-3s^2)q^4)B_0(q^2,m_W^2,m_W^2)-3(5m_Z^2+m_h^2+q^2)A_0(m_h^2)\\
&+3(5m_Z^2+m_h^2-q^2)A_0(m_Z^2)+6(12m_W^2+(9s^2-11c^2)q^2)A_0(m_W^2)\\
&\left.+2q^2(3(8s^4-10s^2+1)m_Z^2-3m_h^2+4s^2q^2)\right]
\end{aligned}$$

$\mathcal{O}_W$:

$$\begin{aligned}
\Delta\Pi_{WW} &= \frac{c_W}{\Lambda^2}\frac{1}{16\pi^2}\frac{g^2}{12q^2}\left[12m_W^2\left(m_W^4(m_W^2+m_Z^2+2q^2)-\left(3m_W^2+m_Z^2\right)q^4\right)C_0(0,0,q^2,m_W^2,0,m_Z^2)\right. \qquad \text{(B.17)}\\
&-(m_W^2(m_h^2-m_W^2)^2+q^2(m_h^4+8m_h^2m_W^2-m_W^4)-q^4(2m_h^2+m_W^2)+q^6)B_0(q^2,m_h^2,m_W^2)\\
&-2s^2m_W^2(m_W^2-q^2)^2B_0(q^2,0,m_W^2)+\left(2(s^6-10s^4+24s^2-12)m_W^2m_Z^4\right.\\
&\left.-(4s^6+45s^4-106s^2+52)m_Z^4q^2-2(s^4-10s^2+11)m_Z^2q^4-q^6\right)B_0(q^2,m_W^2,m_Z^2)\\
&+(m_h^2(m_W^2+q^2)-m_W^4+q^4)A_0(m_h^2)\\
&-\left(m_h^2m_W^2-6m_W^2m_Z^2-7m_W^4+\left(m_h^2-5m_Z^2-11m_W^2\right)q^2+22q^4\right)A_0(m_W^2)\\
&+\left(2(5s^4-14s^2+6)m_W^2m_Z^2+(14s^4-45s^2+26)m_Z^2q^2-(23c^2-s^2)q^4\right)A_0(m_Z^2)\\
&\left.+2q^2\left(m_h^2m_W^2-12m_W^2m_Z^2-7m_W^4+(m_h^2+m_W^2+m_Z^2)q^2-\frac{2}{3}q^4\right)\right]\\
\Delta\Pi_{ZZ} &= \frac{c_W}{\Lambda^2}\frac{1}{16\pi^2}\frac{g^2}{12q^2}\left[24m_W^2m_Z^2(m_W^4+m_W^2q^2-c^2(1+c^2)q^4)C_0(0,0,q^2,m_W^2,0,m_W^2)\right. \qquad \text{(B.18)}\\
&+(-m_Z^2(m_Z^2-m_h^2)^2-(m_h^4+8m_h^2m_Z^2-m_Z^4)q^2+(2m_h^2+m_Z^2)q^4-q^6)B_0(q^2,m_h^2,m_Z^2)\\
&-(24m_W^4m_Z^2+4(m_W^2m_Z^2+12m_W^4)q^2+2(8s^4-24s^2+11)m_Z^2q^4\\
&+(c^2-s^2)q^6)B_0(q^2,m_W^2,m_W^2)+(m_h^2m_Z^2-m_Z^4+m_h^2q^2+q^4)A_0(m_h^2)\\
&+(m_Z^4-m_h^2m_Z^2-(10m_Z^2+m_h^2)q^2+q^4)A_0(m_Z^2)\\
&+2(12m_W^2m_Z^2+2(m_Z^2+12m_W^2)q^2-(13+10c^2)q^4)A_0(m_W^2)\\
&\left.+q^2\left(2m_h^2m_Z^2-2(24s^4-44s^2+19)m_Z^4+(2m_h^2+4(c^2-s^2)m_W^2)q^2-\frac{4c^2}{3}q^4\right)\right]\\
\Delta\Pi_{\gamma\gamma} &= -\frac{c_W}{\Lambda^2}\frac{1}{16\pi^2}\frac{g^2q^2s^2}{6}\left[12m_W^4C_0(0,0,q^2,m_W^2,0,m_W^2)+(8m_W^2+q^2)B_0(q^2,m_W^2,m_W^2)\right. \qquad \text{(B.19)}\\
&\left.+10A_0(m_W^2)-4m_W^2+\frac{2q^2}{3}\right]\\
\Delta\Pi_{\gamma Z} &= \frac{c_W}{\Lambda^2}\frac{1}{16\pi^2}\frac{g^2s}{72c}\left[-72(1+2c^2)m_W^4q^2C_0(0,0,q^2,m_W^2,0,m_W^2)\right. \qquad \text{(B.20)}\\
&+3((m_Z^2-m_h^2)(5m_Z^2+m_h^2)+(2m_h^2-4m_Z^2)q^2-q^4)B_0(q^2,m_h^2,m_Z^2)\\
&-3(48m_W^4+16(1+2c^2)m_W^2q^2+(3c^2-s^2)q^4)B_0(q^2,m_W^2,m_W^2)\\
&+3(m_h^2+5m_Z^2+q^2)A_0(m_h^2)-3(m_h^2+5m_Z^2-q^2)A_0(m_Z^2)\\
&+6(24m_W^2-(13+20c^2)q^2)A_0(m_W^2)\\
&\left.-2(72m_W^4-3((8s^4-14s^2+7)m_Z^2+m_h^2)q^2+4c^2q^4)\right]
\end{aligned}$$

$\mathcal{O}_{WWW}$:

$$\begin{aligned}
\Delta\Pi_{WW} &= \frac{c_{WWW}}{\Lambda^2}\frac{1}{16\pi^2}3g^4\left[2m_W^4(m_W^2-q^2)C_0\left(0,0,q^2,m_W^2,0,m_Z^2\right)\right. \qquad \text{(B.21)}\\
&+m_Z^2\left((s^2-2c^2)m_W^2-c^2q^2\right)B_0\left(q^2,m_W^2,m_Z^2\right)-\left((s^2-c^2)m_W^2+2c^2q^2\right)A_0\left(m_Z^2\right)\\
&\left.+\left(m_W^2-2q^2\right)A_0(m_W^2)+\frac{3}{2}m_W^2q^2+\frac{q^4}{6}\right]\\
\Delta\Pi_{ZZ} &= \frac{c_{WWW}}{\Lambda^2}\frac{1}{16\pi^2}3g^4\left[2m_W^4(m_W^2-c^2q^2)C_0\left(0,0,q^2,m_W^2,0,m_W^2\right)\right. \qquad \text{(B.22)}\\
&-m_W^2(2m_W^2+(c^2-s^2)q^2)B_0\left(q^2,m_W^2,m_W^2\right)+2(m_W^2-2c^2q^2)A_0\left(m_W^2\right)\\
&\left.+\frac{1}{2}m_W^2(3c^2-s^2)q^2+\frac{1}{6}c^2q^4\right]\\
\Delta\Pi_{\gamma\gamma} &= -\frac{c_{WWW}}{\Lambda^2}\frac{1}{16\pi^2}6g^4q^2s^2\left[m_W^4C_0\left(0,0,q^2,m_W^2,0,m_W^2\right)+m_W^2B_0\left(q^2,m_W^2,m_W^2\right)\right. \qquad \text{(B.23)}\\
&\left.+2A_0(m_W^2)-m_W^2-\frac{q^2}{12}\right]\\
\Delta\Pi_{\gamma Z} &= \frac{c_{WWW}}{\Lambda^2}\frac{1}{16\pi^2}\frac{3g^4}{2}\frac{s}{c}\left[2m_W^4(m_W^2-2c^2q^2)C_0(0,0,q^2,m_W^2,0,m_W^2)\right. \qquad \text{(B.24)}\\
&-m_W^2(2m_W^2+(3c^2-s^2)q^2)B_0(q^2,m_W^2,m_W^2)+2(m_W^2-4c^2q^2)A_0(m_W^2)\\
&\left.+\frac{1}{2}m_W^2(7c^2-s^2)q^2+\frac{c^2q^4}{3}\right]
\end{aligned}$$

References

[1] B. Grzadkowski, M. Iskrzynski, M. Misiak, and J. Rosiek, JHEP **1010**, 085 (2010).

[2] K. Hagiwara, S. Ishihara, R. Szalapski, and D. Zeppenfeld, Phys.Rev. **D48**, 2182 (1993).

[3] K. Gaemers and G. Gounaris, Z.Phys. **C1**, 259 (1979).

[4] J. Beringer et al., Phys.Rev. **D86**, 010001 (2012).

[5] D. Zeppenfeld and S. Willenbrock, Phys.Rev. **D37**, 1775 (1988).

[6] W. Kilian, T. Ohl, and J. Reuter, Eur.Phys.J. **C71**, 1742 (2011).

[7] J. Alwall, M. Herquet, F. Maltoni, O. Mattelaer, and T. Stelzer, JHEP **1106**, 128 (2011).

[8] A. De Rujula, M. Gavela, P. Hernandez, and E. Masso, Nucl.Phys. **B384**, 3 (1992).

[9] K. Hagiwara, S. Ishihara, R. Szalapski, and D. Zeppenfeld, Phys.Lett. **B283**, 353 (1992).

[10] D. Kennedy and B. Lynn, Nucl.Phys. **B322**, 1 (1989).

[11] M. E. Peskin and T. Takeuchi, Phys.Rev.Lett. **65**, 964 (1990).

[12] M. E. Peskin and T. Takeuchi, Phys.Rev. **D46**, 381 (1992).

[13] M. Gonzalez-Garcia, S. Lietti, and S. Novaes, Phys.Rev. **D59**, 075008 (1999).

[14] M. Gonzalez-Garcia, Int.J.Mod.Phys. **A14**, 3121 (1999).

[15] T. Corbett, O. Eboli, J. Gonzalez-Fraile, and M. Gonzalez-Garcia, Phys.Rev. **D86**, 075013 (2012).

[16] T. Corbett, O. Eboli, J. Gonzalez-Fraile, and M. Gonzalez-Garcia, Phys.Rev. **D87**, 015022 (2013).

[17] S. Alam, S. Dawson, and R. Szalapski, Phys.Rev. **D57**, 1577 (1998).

[18] S. Schael et al., Eur.Phys.J. **C49**, 411 (2007).

[19] S. Schael et al., (2013).

[20] C. Grojean, E. E. Jenkins, A. V. Manohar, and M. Trott, (2013).

[21] R. Mertig, M. Bohm, and A. Denner, Comput.Phys.Commun. **64**, 345 (1991).

[22] T. Hahn and M. Perez-Victoria, Comput.Phys.Commun. **118**, 153 (1999).